Evidence for *FHL1* as a novel disease gene for isolated hypertrophic cardiomyopathy

Felix W. Friedrich[1], Brendan R. Wilding[2], Silke Reischmann[1], Claudia Crocini[1], Patrick Lang[3], Philippe Charron[4,5,8], Oliver J. Müller[9], Meagan J. McGrath[2], Ingra Vollert[1], Arne Hansen[1], Wolfgang A. Linke[3], Christian Hengstenberg[10], Gisèle Bonne[5,6,7], Stellan Morner[11], Thomas Wichter[12,†], Hugo Madeira[13], Eloisa Arbustini[14], Thomas Eschenhagen[1], Christina A. Mitchell[2], Richard Isnard[4,8] and Lucie Carrier[1,5,6,*]

[1]Department of Experimental Pharmacology and Toxicology, Cardiovascular Research Center, University Medical Center Hamburg-Eppendorf, Hamburg, Germany, [2]Faculty of Medicine, Nursing and Health Sciences, Department of Biochemistry and Molecular Biology, Monash University, Clayton, Australia, [3]Department of Cardiovascular Physiology, Ruhr University Bochum, Bochum, Germany, [4]Inserm, U956, [5]UPMC Univ Paris 06, IFR14, [6]Inserm U974, CNRS UMR7215, Institut de Myologie, [7]AP-HP, Unité Fonctionnelle de Cardiogénétique et Myogénétique, Service de Biochimie Métabolique and [8]AP-HP, Centre de référence des maladies cardiaques héréditaires, Groupe Hospitalier Pitié-Salpêtrière, Paris F-75013, France, [9]Department of Cardiology, Internal Medicine III, University Hospital Heidelberg, Heidelberg, Germany, [10]Klinik und Poliklinik für Innere Medizin II, Universitätsklinikum Regensburg, Regensburg, Germany, [11]Department of Public Health and Clinical Medicine, Umeå University, Umeå, Sweden, [12]Department of Cardiology and Angiology, University Hospital Münster, Münster, Germany, [13]Serviço de Cardiologia, Santa Maria Hospital, Lisbon, Portugal and [14]Centre for Inherited Cardiovascular Diseases, Istituto Di Ricovero e Cura a Carattere Scientifico (IRCCS), Fondazione Policlinico San Matteo, Pavia, Italy

Hypertrophic cardiomyopathy (HCM) is characterized by asymmetric left ventricular hypertrophy, diastolic dysfunction and myocardial disarray. HCM is caused by mutations in sarcomeric genes, but in >40% of patients, the mutation is not yet identified. We hypothesized that *FHL1*, encoding four-and-a-half-LIM domains 1, could be another disease gene since it has been shown to cause distinct myopathies, sometimes associated with cardiomyopathy. We evaluated 121 HCM patients, devoid of a mutation in known disease genes. We identified three novel variants in *FHL1* (c.134delA/K45Sfs, c.459C>A/C153X and c.827G>C/ C276S). Whereas the c.459C>A variant was associated with muscle weakness in some patients, the c.134delA and c.827G>C variants were associated with isolated HCM. Gene transfer of the latter variants in C2C12 myoblasts and cardiac myocytes revealed reduced levels of FHL1 mutant proteins, which could be rescued by proteasome inhibition. Contractility measurements after adeno-associated virus transduction in rat-engineered heart tissue (EHT) showed: (i) higher and lower forces of contraction with K45Sfs and C276S, respectively, and (ii) prolonged contraction and relaxation with both mutants. All mutants except one activated the fetal hypertrophic gene program in EHT. In conclusion, this study provides evidence for *FHL1* to be a novel gene for isolated HCM. These data, together with previous findings of proteasome impairment in HCM, suggest that FHL1 mutant proteins may act as poison peptides, leading to hypertrophy, diastolic dysfunction and/or altered contractility, all features of HCM.

*To whom correspondence should be addressed at: Department of Experimental Pharmacology and Toxicology, Cardiovascular Research Center, University Medical Center Hamburg-Eppendorf, Martinistraße 52, D-20246 Hamburg, Germany. Tel: +49 40741057208; Fax: +49 40741055925; Email: l.carrier@uke.de
†Present address: Department of Cardiology, Marienhospital Osnabrück, Heart Center Osnabrück-Bad Rothenfelde, Osnabrück, Germany.

Table 1. *FHL1* genetic variants identified in patients with HCM

Variant #no.	Localization	Genetic change	Codon change	Amino acid exchange
I	Exon 3	c.134delA	AGC>GCC	p.Ser45fs (K45Sfs)
II	Exon 5	c.459C>A	TGC>TGA	p.Cys153X (C153X)
III	Exon 8	c.827G>C	TGT>TCT	p.Cys276Ser (C276S)
IV	Exon 8	rs151315725, c.823G>A	GAC>AAC	p.Asp275Asn (D275N)
V	Exon 5	rs149670651, c.441C>T	GAC>GAT	p.Asp147Asp (D147D)

INTRODUCTION

Four-and-a-half LIM domains 1 (FHL1) is a member of the FHL protein family, composed of FHL 1, 2, 3, 4 and ACT (activator of CREM), and characterized by an N-terminal half LIM domain followed by four complete LIM domains (reviewed in [1]). The LIM domain is a double-zinc finger protein-binding motif, named according to its initial discovery in the proteins Lin11, Isl-1 and Mec-3 [2]. FHL proteins are localized within the cytoskeleton and the nucleus and can shuttle between these compartments [3–5]. FHL1 is the main isoform of striated muscles and has been suggested to contribute to sarcomere synthesis, assembly and biomechanical stress sensing [6,7].

FHL1 has been shown to bind different partners, including sarcomeric proteins such as the slow-skeletal myosin-binding protein C (MyBP-C) or titin [7,8], the potassium channel KCNA5 in human atrium [9] and the calcineurin-dependent nuclear factor of activated T cells, cytoplasmic 1 (NFATc1; [10]). Three isoforms of FHL1 are generated by alternative splicing [1]. FHL1A, also recognized as skeletal muscle LIM protein 1, is the full-length protein expressed in many cell types, with highest levels in skeletal muscle, intermediate levels in the heart and low expression in placenta, ovary, prostate, testis, small intestine, colon and spleen [3]. FHL1B, or SLIMMER, contains the LIM domains 1–3 plus nuclear localization and export signals, as well as an RBP-J binding region, and is expressed in brain, skeletal muscle and, to a lesser extent, in heart, colon, prostate and small intestine [3]. The shortest isoform, FHL1C or KyoT2, contains only the LIM domains 1 and 2 plus an RBP-J binding region, but no nuclear localization signal [11]. In comparison to FHL1A, it is expressed at much lower levels in heart, testis and skeletal muscle [12].

FHL1 gene mutations cause distinct X-linked skeletal muscle disorders such as X-linked myopathy with postural muscle atrophy with generalized hypertrophy (XMPMA; [13]), reducing body myopathy (RBM; [14,15]), scapuloperoneal myopathy (SPM; [16]) and Emery–Dreifuss muscular dystrophy (EDMD; [17]). In several cases, a cardiac phenotype has been observed (reviewed in [1]), including mainly arrhythmias, but also hypertrophic cardiomyopathy (HCM) or dilated cardiomyopathy (DCM). HCM has been specifically reported in *FHL1* carriers presenting with XMPMA or EDMD [13,17,18]. Interestingly, the expression of the *FHL1* gene is upregulated in human HCM [19,20] and in experimental models of cardiac hypertrophy induced by pressure overload or β-adrenergic agonists [6,21].

HCM is characterized by asymmetric left ventricular (LV) hypertrophy, diastolic dysfunction and increased interstitial fibrosis [22,23]. The phenotype can be very variable. Many patients are asymptomatic or only slightly symptomatic. Symptoms include dyspnea, chest pain, palpitations, light-headedness, fatigue and syncope. The disease may evolve toward sudden cardiac death, particularly in young athletes or heart failure. HCM is a genetic disease, mainly transmitted as an autosomal dominant trait, but also with X-linked patterns, and is caused by mutations in at least 14 genes encoding components of the sarcomere (reviewed in [24–27]). The genes *MYH7* encoding β-myosin heavy chain and *MYBPC3* encoding cardiac MyBP-C (cMyBP-C) are the most frequently mutated, accounting for ∼80% of the mutations causing HCM [24]. Still, a considerable number (∼40%) of HCM patients do not carry mutations in any of the already established HCM disease genes, suggesting mutations in so far not identified genes. For example, X-linked mutations in *LAMP2*, encoding the lysosomal-associated membrane protein 2, have also been shown to cause Danon disease presenting with HCM [28,29]. We hypothesized that *FHL1*, located on the Xq26.3 chromosome, could be another HCM disease gene and performed a screen for *FHL1* mutations in a cohort of HCM patients devoid of mutations in established disease genes. We identified five different *FHL1* genetic variants and analyzed their impact after gene transfer in different cell types, in binding assays with isolated human cardiac myofibrils and on contractility measurements in rat-engineered heart tissue (EHT).

RESULTS

Identification of *FHL1* variants in patients with HCM

We enrolled in this study 121 HCM index cases who do not carry a mutation in five of the previously described HCM disease genes. The screening of *FHL1* for mutations led to the identification of three novel and two previously reported *FHL1* variants (Table 1 and Figs. 1 and 2). The *FHL1* variants were found in seven unrelated families from France, Germany, Italy, Portugal and Sweden. All but one of the index cases presented with a clear septal and/or posterior wall hypertrophy, and the Portuguese proband had apical HCM; in some cases, an abnormal electromyogram (EMG) and a muscular phenotype were associated (Table 2). Due to the small size of the investigated HCM families, X-linked transmission could not be fully validated from the pedigrees, but was compatible with data obtained from the seven available pedigrees (Fig. 1).

Variant I is a one-nucleotide deletion (c.134delA) in exon 3, affecting the three FHL1 isoforms and resulting in a frameshift and a C-terminal truncated protein (K45Sfs) of 16.3 kDa, lacking at least the LIM2, LIM3 and LIM4 domains. It was
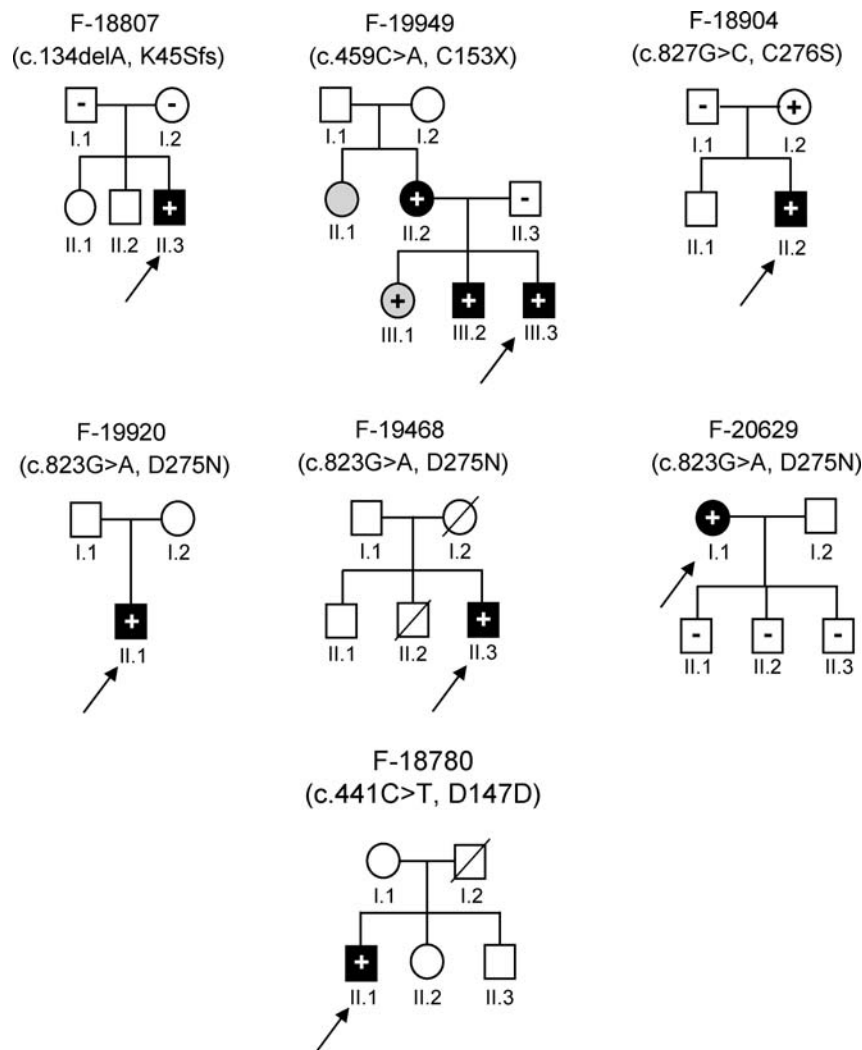
Figure 1. Pedigrees of families with HCM carrying *FHL1* variants. *FHL1* variants were found in seven unrelated families from Italy, France, Germany, Portugal and Sweden. D275N was found in three families, whereas the other variants were only detected in one family. Roman numerals symbolize generations. Arabic numerals mark individuals within each generation. Males are symbolized as squares and females as circles. Individuals with HCM are indicated by black symbols, individuals with an intermediate phenotype by gray symbols, unaffected individuals by empty symbols and deceased individuals by a diagonal line. Index cases are indicated by the arrows. Family members with a plus sign (+) carry the respective mutation; non-carriers are marked with a minus sign (−) and individuals without signs were not genotyped.

detected in an Italian single case (II.3, F-18807), who was diagnosed as a young adult with septal hypertrophy and outflow tract obstruction. His parents (I.1 and I.2) do not carry the variant and are not clinically affected, suggesting a de novo mutation. The sister (II.1) and brother (II.2) of the index case could not be genetically evaluated, but both were not clinically affected. No family history of muscular disease has been reported.

Variant II is a nonsense point mutation (c.459C>A) in exon 5, affecting the three FHL1 isoforms. It results in a truncated protein (C153X) of 17.5 kDa, lacking the LIM3 and LIM4 domains. It was detected in four individuals of a French family (F-19949). Already at the age of 13, the index case (III.3) was diagnosed with HCM. He also presented with muscular symptoms, such as Achilles tendon contractures and respiratory insufficiency due to diaphragm weakness. A skeletal muscle biopsy showed mild neuropathic features, and creatine

kinase levels were normal. At the age of 19, heart transplantation was required because of congestive heart failure (pulmonary edema). His brother (III.2) was also diagnosed with HCM at the age of 10. At the age of 5, he had already presented with skeletal muscle weakness and walking difficulty, but over the years, he showed a good evolution with no major muscle problem, except for rare myalgia, mild difficulty in heel walking and hypophonia, which were possibly of muscular origin. Interestingly, the mother (II.2) and the sister (III.1) of the index case, who are heterozygotes for the mutation, both have HCM diagnosed by echocardiography or by electrocardiogram (ECG; Table 2). Finally, the aunt of the index case (II.1) presented with an intermediate phenotype, characterized by a borderline septal hypertrophy and normal ECG, but she was not available for genetic screening.

Variant III is a missense point mutation (c.827G>C) located in exon 8, affecting only the FHL1A isoform.
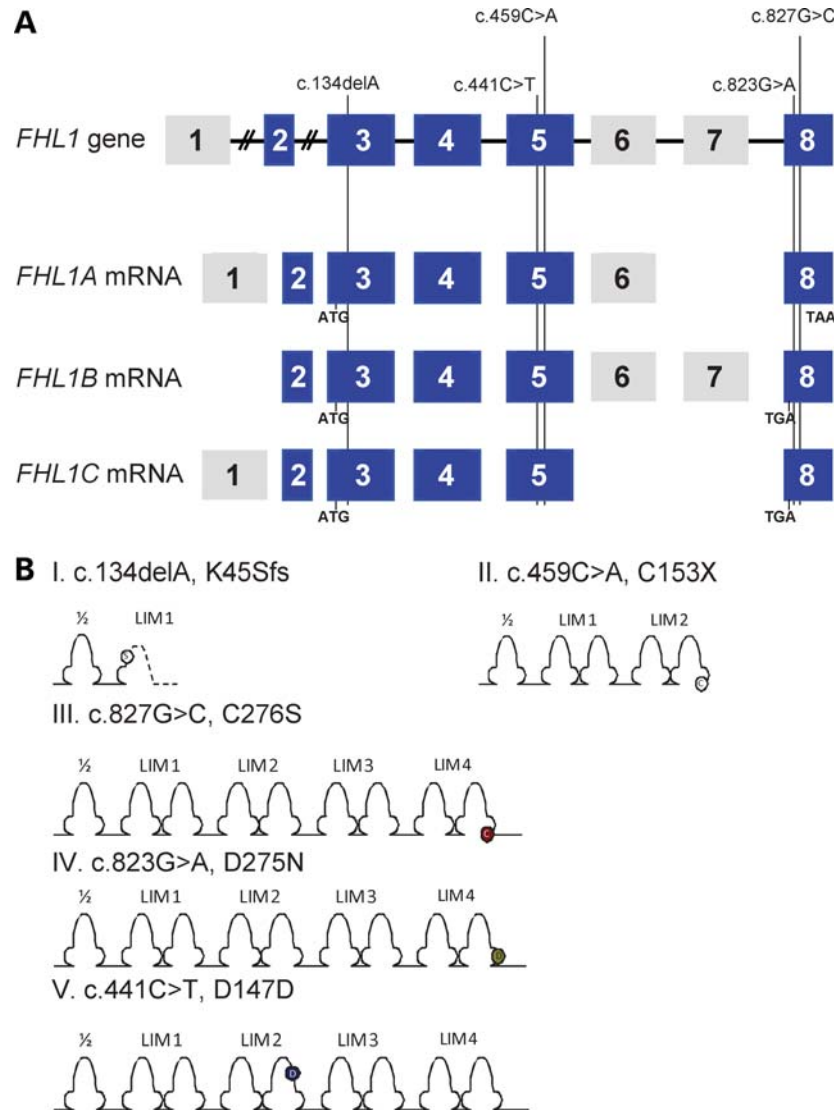
Figure 2. Variants in the *FHL1* gene and mRNAs and their impact on protein structure. (**A**) Human *FHL1* gene consists of eight exons. Exons 1 and 2 are non-coding, whereas exons 3–8 give rise to three mRNA isoforms by alternative splicing: *FHL1A*, *FHL1B* and *FHL1C*. Light gray squares represent alternative spliced exons. Translational start (ATG) and stop (TAA or TGA) codons are indicated for the three *FHL1* isoforms. The five *FHL1* variants identified in HCM patients are depicted; they were located in exons 3, 5 and 8 and are frame shift, nonsense, missense or silent mutations. (**B**) Impact of the different genetic variants on the FHL1A protein LIM domain structure.

It leads to a full-length mutant protein (C276S) of 31.9 kDa. It was detected in an Italian patient (II.2, F-18904), presenting with a 22 mm septal wall thickness at the age of 18 (Table 2). Diagnosis of HCM was made in his adolescence. He did not present with other clinical symptoms, especially no muscle weakness or signs of myopathy. His mother carries the variant, but was clinically unaffected; his father was genetically and phenotypically unaffected.

Variant IV is a missense point mutation (c.823G>A) located in exon 8, resulting in a full-length mutant FHL1A protein (D275N) of 31.9 kDa. It was found independently in three families from Sweden, Portugal and Germany. Besides a clear HCM phenotype, no muscle phenotype was reported for the Swedish and Portuguese patients. The female Portuguese patient (I.1, F-20629) has an apical wall thickness of

17 mm and did not transmit the variant to her three sons (Fig. 1 and Table 2). The German patient (II.3, F-19468), in contrast, showed a muscle phenotype and complained of general weakness and atrophy of the lower legs. Electromyography examination showed neuromuscular patterns, which could also be explained by a history of poliomyelitis in childhood.

Variant V is a silent point mutation (c.441C>T) located in exon 5, which is expected to produce an FHL1A synonymous wild-type (WT) protein (D147D) of 31.9 kDa. It was found in a German patient (II.1, F18780) presenting with a septal wall thickness of 16 mm (Table 2). His father received a pacemaker in the 1970s and died suddenly in his mid-30s. His mother has no known cardiac disease. Both his sister and his brother are healthy. No structural heart disease has been diagnosed.

Table 2. Clinical and genetic features of HCM index cases and relatives

Family	Ind	Sex	Birth year	Age at diagnosis	Proband	Clinical status	Age at onset	PWth (mm)	SWth (mm)	ECG	Muscle phenotype	CK	Other symptoms	Var	FHL1 variant	Genetic status	FHL1 protein consequence
18807	II.3	M	1985	17	P	A	16	16	20	Abnormal	No	Normal	No	I	c.134delA	Hem	p.Ser45fs
	I.1	M	1957	45		NA					No		No		No		
	I.2	F	1959	43		NA					No		No		No		
19949	III.3	M	1984	18	P	A	HCM age 13, heart transplant age 19	13	29	Abnormal	Diaphragm weakness, EMG almost normal, Achilles tendon contractures, neuropathic features in biopsy	Normal	No	II	c.459C>A	Hem	p.Cys153X
	II.2	F	1959	43		A		8	17	Abnormal	No	Normal	No		c.459C>A	Het	p.Cys153X
	II.3	M	1955	47		NA		9	10	Normal	No		No		No		
	III.2	M	1988	14		A	10	8	16	Abnormal	Difficulties walking on heels	Normal	Myalgia, hypophonia		c.459C>A	Hem	p.Cys153X
	III.1	F	1997	5		I		3	5	Abnormal	No		No		c.459C>A	Het	p.Cys153X
18904	II.2	M	1979	23	P	A	18	12	20	Normal	No	Normal	No	III	c.827G>C	Hem	p.Cys276Ser
	I.1	M	1948	54		NA		7	8		No		No		No		
	I.2	F	1949	53		NA		7	8	Normal	No		No		c.827G>C	Het	p.Cys276Ser
20629	I.1	F	1955	47	P	A	47	10	10	Abnormal	No		No	IV	c.823G>A	Het	p.Asp275Asn
	II.1	M	1979	23		NA		10.8	10.8	Normal	No		No		No		
	II.2	M	1981	21		NA		7.8	9.3	Normal	No		No		No		
	II.3	M	1985	17		NA		7.8	12.6	Normal	No		No		No		
19920	II.1	M	1924	78	P	A	78	11	20	Normal	No	Normal	No	IV	c.823G>A	Hem	p.Asp275Asn
19468	II.3	M	1940	62	P	A	49	19	24	Abnormal	General weakness, abnormal EMG		Poliomyelitis in childhood	IV	c.823G>A	Hem	p.Asp275Asn
18780	II.1	M	1969	33	P	A	22	14	16	Abnormal	No		No	V	c.441C>T	Hem	p.Asp147Asp

A, affected; CK, creatine kinase; F, female; Hem, hemizygote; Het, heterozygote; I, intermediate; Ind, individual number; M, male; P, proband; NA, not affected; PWth, posterior wall thickness; SWth, septal wall thickness; Var, variant number. Abnormal ECG corresponds to abnormal negative T-waves.

None of the family members exhibits signs of a neuromuscular disorder.

None of the variants was detected in 285 control individuals. However, variant IV has been found in 3 of 247 control individuals in a previous study (30) and was previously reported as a single nucleotide polymorphism (SNP) with an allele frequency of 1.2% (rs151315725). This non-synonymous variant is predicted as benign by PolyPhen and as tolerated by SIFT. Variant V is synonymous and has also been reported as a rare SNP with an allele frequency of 0.2% (rs149670651). Variants IV and V were therefore considered polymorphisms, likely unrelated to disease.

FHL1 variants associated with HCM are expressed at low levels in C2C12 myoblasts

The c.459C>A and c.134delA *FHL1* variants are predicted to result in large C-terminal truncation and hence loss of normal FHL1 protein function affecting all three isoforms (Fig. 2B). Therefore, we first analyzed the expression of these two *FHL1* variants at the protein level (K45Sfs and C153X) after gene transfer in C2C12 myoblasts and compared them with the expression of *FHL1* WT. We also compared with the expression of *FHL1* missense mutations that have been shown to cause the skeletal muscle wasting diseases RBM (C132F, 102–104delKFC, 151–153delVTC), SPM (W122S), XMPMA (127-I-128, C224W) and EDMD (C276Y; Fig. 3). All proteins were detected migrating at the predicted molecular weight, but the level of both HCM-associated truncated mutants was much lower than that of WT or the other mutants (Fig. 3A). Gene transfer with different amounts of cDNA further confirmed the lower levels of HCM-associated mutants than of WT or RBM^C132F-associated mutant (Supplementary Material, Fig. S1).

Low levels of mutant proteins could be the result of reduced translation or accelerated protein degradation. We therefore investigated whether HCM-associated FHL1 mutants are degraded by the ubiquitin–proteasome system (UPS), which is considered to be the major proteolytic system (31,32). Twenty-four hours before myoblasts were harvested, the proteasome inhibitor MG132 or the vehicle dimethyl sulfoxide (DMSO) was applied. Whereas FHL1 WT and RBM^C132F protein levels were not affected by the treatment, protein levels of both HCM-truncated mutants were markedly higher after MG132 treatment (Fig. 3B). Similar results were observed after transfection of COS-1 cells (Supplementary Material, Fig. S2). Interestingly, the lysosome inhibitor bafilomycin A1 also increased the levels of HCM-truncated mutants after gene transfer in COS-1 cells (Supplementary Material, Fig. S2).

We then evaluated the expression level and localization of the different HA-tagged FHL1 mutants by immunofluorescence analysis after transfection of C2C12 myoblasts (Fig. 4). In the absence of the proteasome inhibitor, the number of HA-positive myoblasts was >90% lower with HCM mutants than with WT or RBM^C132F mutant. After MG132 treatment, the number of HA-positive cells of HCM mutants increased to reach 50% of the WT number (Fig. 4A and B), and HA-FHL1 WT and mutants were mainly located in the cytoplasm of myoblasts (Fig. 4C).
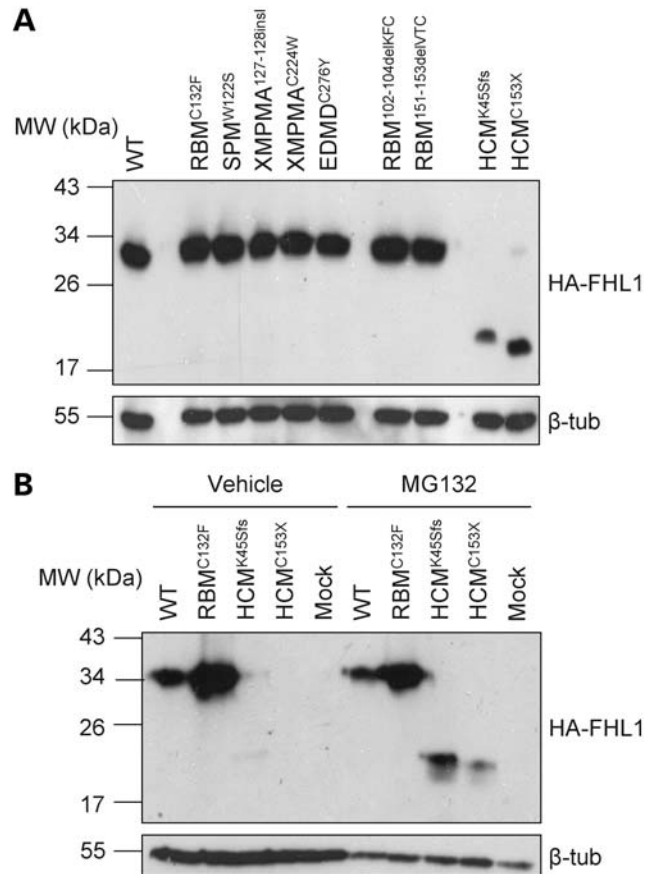
Figure 3. Protein levels of FHL1 WT and mutants after gene transfer in C2C12 myoblasts. C2C12 myoblasts were transfected with plasmid cDNA encoding HA-tagged WT or FHL1A mutants for 4 h. (**A**) Western blots were stained with antibodies directed against the HA-FHL1 or β-tubulin (β-tub) of proteins extracted from C2C12 myoblasts transfected with 4 μg plasmid. Blot shows HA-FHL1 WT and mutants identified in RBM (RBM^C132F and RBM^102–104delKFC), SPM (SPM^W122S), X-linked myopathy with postural muscle atrophy and generalized hypertrophy (XMPMA^127–128insl and XPMA^C224W), EDMD (EDMD^C276Y) and HCM (HCM^K45Sfs and HCM^C153X). (**B**) Western blot stained with the HA and the β-tub antibodies directed against proteins extracted from C2C12 myoblasts transfected with 1 μg HA-FHL1 WT, mutants or Mock, and treated for 24 h with 20 μM MG132 in 0.1% DMSO or with vehicle alone. MG132 partially increased the level of HCM-truncated mutants. The migration of protein molecular weight (MW) markers is indicated.

Both WT and mutant FHL1 proteins bind to the I-band region of human cardiac myofibrils

FHL1 has been shown to mainly localize to the sarcomeric I-band, but also to a lesser extent to the M-band of the sarcomere in skeletal myocytes (8). We first evaluated the localization of FHL1 in neonatal mouse cardiac myocytes (NMCMs) and adult mouse ventricular myocytes (AMVMs; Fig. 5). In NMCMs, FHL1 showed a striated pattern, which was in alternation with the striated pattern of cMyBP-C located in the A-band of the sarcomere (Fig. 5A), therefore consistent with an I-band localization of FHL1. In AMVMs, co-staining with an antibody directed against the Z1 domain of titin in the Z-disk revealed co-localization of both proteins at the short sarcomere lengths typical for these cell cultures (Fig. 5B).
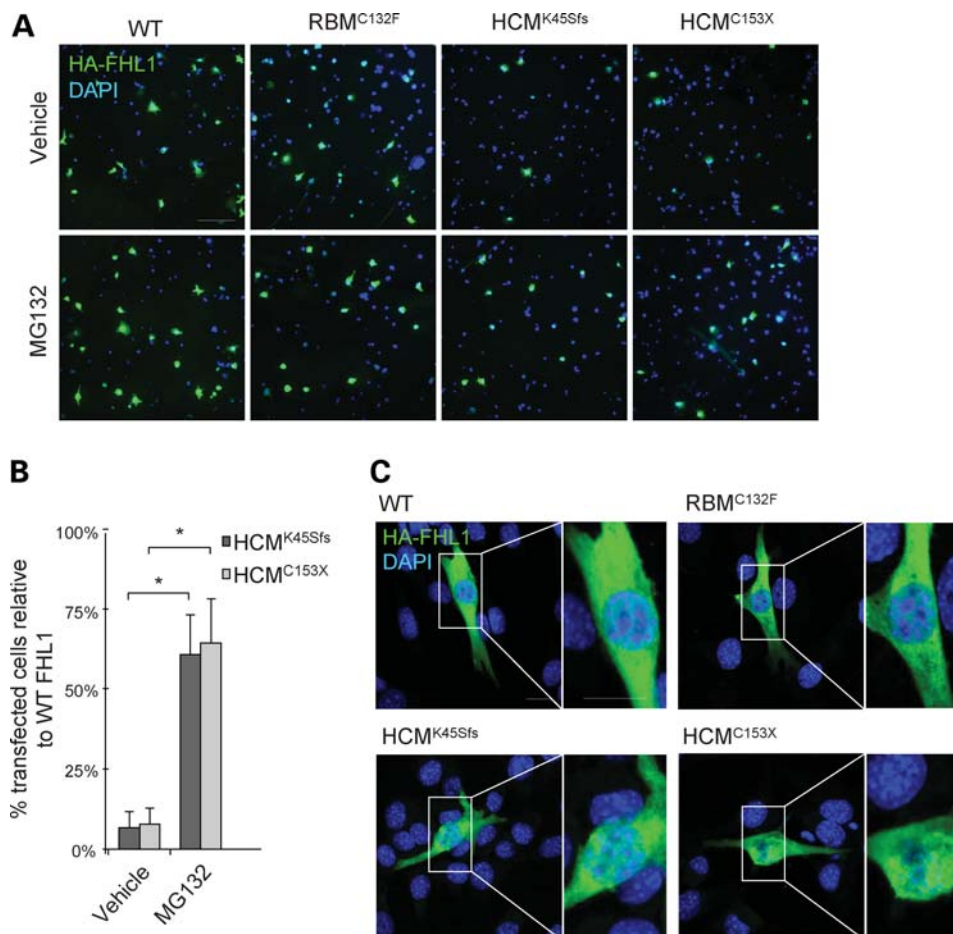
Figure 4. Immunofluorescence analysis of FHL1 WT and mutants after gene transfer in C2C12 myoblasts. C2C12 myoblasts were transfected with 1 μg of plasmid cDNA encoding HA-tagged WT FHL1 or FHL1 mutants for 4 h and then treated for 24 h with 20 μM MG132 in 0.1% DMSO or with vehicle alone. Cells were then fixed and stained with the HA antibody recognizing HA-FHL1 WT and mutants found in RBM (RBM[C132F]) or in HCM (HCM[K45Sfs] and HCM[C153X]). Cells were also stained with DAPI to mark the nuclei. (**A**) Representative immunofluorescence images of FHL1 WT and mutants obtained after vehicle or MG132 treatment. (**B**) Percentage of HA-positive myoblasts (related to HA-FHL1 WT 100%) observed after transfection with the HA-FHL1 HCM mutants, and obtained in the absence (vehicle), or after MG132 treatment. Data are expressed as mean ± SEM, with $^*P < 0.05$ versus vehicle ($n = 3$), Student's *t*-test. (**C**) Confocal image micrographs of transfected C2C12 myoblasts treated with MG132, showing that cytoplasmic localization of HA-FHL1 mutants did not differ from the WT. Right panels correspond to higher magnifications of left panels. Scale bars: 100 μm in (A) and 20 μm in (C).

We then evaluated whether FHL1 WT and mutants bind to human cardiac myofibrils *ex vivo*. Whereas recombinant WT, C153X, C276S and D275N proteins were expressed in bacteria, recombinant K45Sfs could not be produced, possibly due to misfolding and poison peptide effect on bacterial growth. For the binding assay, isolated and stretched human cardiac myofibrils were incubated with recombinant FHL1 proteins and immunostained for FHL1. Comparison of fluorescence and phase images revealed binding of the FHL1 WT protein to the I-band region of the sarcomere (Fig. 6), confirming and extending previous findings of an interaction between FHL1 and the N2B region of titin *in vitro* (7). Specifically, FHL1 appeared as tightly spaced double bands flanking sarcomeric Z-disks. All three FHL1 mutants showed I-band staining as well, but double bands were less clearly distinguishable than with the WT protein, suggesting a lower binding specificity. Myofibrils that were not incubated with recombinant FHL1 did not exhibit the I-band doublet signals (Fig. 6).

FHL1 mutants are degraded by the UPS after gene transfer in cardiac myocytes

We then investigated whether *FHL1* variants are stably expressed after gene transfer in cardiac myocytes. NMCMs were transduced with adeno-associated virus serotype 6 (AAV-6) encoding FLAG-tagged FHL1 WT, truncated or full-length HCM mutants (K45Sfs, C153X, C276S and D275N) at a multiplicity of infection (MOI) of 10 000 for 48 h and then exposed to 1 μM MG132 or vehicle for 24 h. Western blot analysis was performed using antibodies directed against the FLAG epitope and β-actin, which was used as a loading control (Fig. 7A). As in C2C12 myoblasts and in COS-1 cells, protein levels of the truncated K45Sfs and C153X mutants were much lower than those of WT (Fig. 7A). Interestingly, the C276S full-length mutant was also barely detectable, whereas the protein level of D275N, which is considered a polymorphism (30), did not differ from the WT (Fig. 7A).
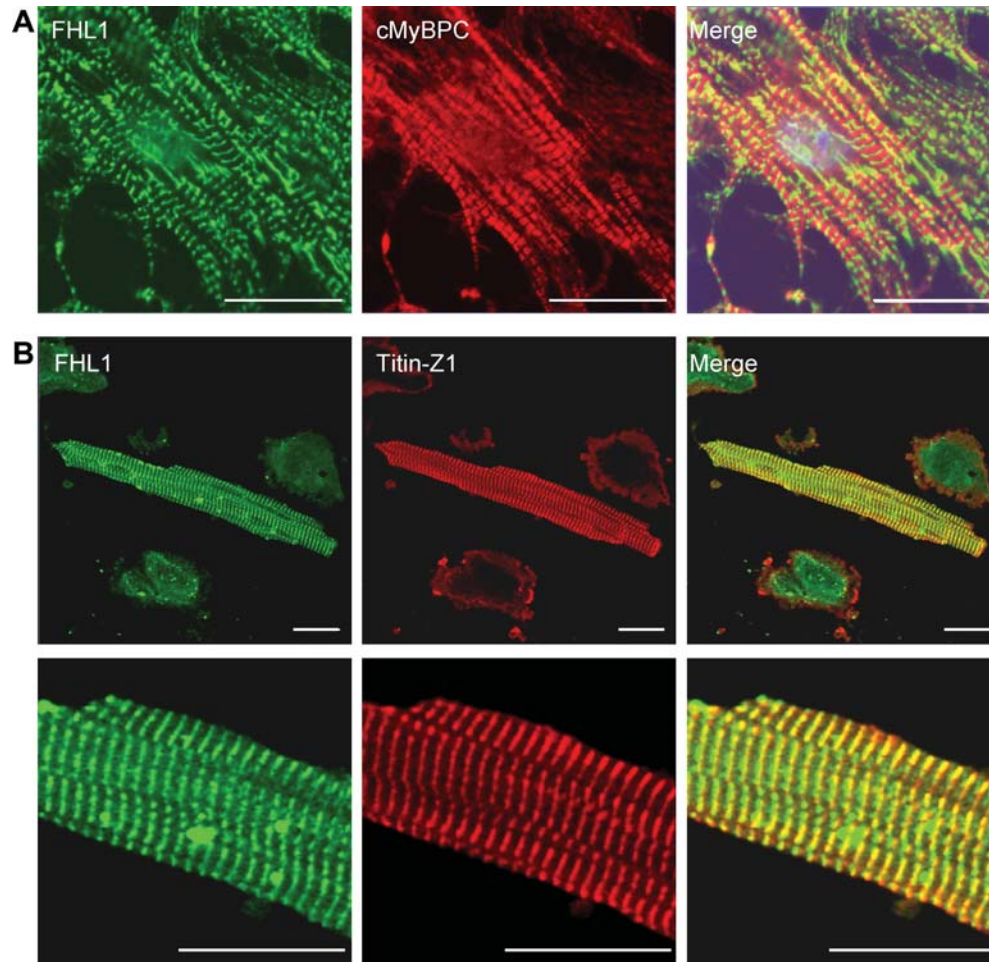
Figure 5. Immunofluorescence images of native FHL1 in mouse cardiac myocytes. (**A**) Cardiac myocytes were isolated from neonatal mice, fixed and stained with antibodies directed against FHL1 (green) or cMyBP-C (red). (**B**) Ventricular myocytes were isolated from an adult mouse, fixed and stained with antibodies directed against FHL1 (green) and the Z1 domain of titin (titin-Z1, red). Lower panel is a magnification of the upper panel. Scale bar: 20 μm.

Inhibition of the proteasome with MG132 markedly increased the levels of truncated and full-length HCM mutants, but did not affect the protein levels of WT or D275N mutant (Fig. 7A and B).

Further, we studied the localization of FHL1 WT and mutants after AAV-6 transduction of cardiac myocytes followed by treatment with MG132 (Fig. 8). FLAG-tagged FHL1 WT, C276S and D275N proteins exhibited a striated pattern in alternation with cMyBP-C. Only a few myocytes showed FLAG-tagged FHL1-truncated mutants. In those rare cases, however, the K45Sfs and C153X mutants were not well incorporated into the sarcomere and showed a patchy pattern indicating aggregates (Fig. 8).

### K45Sfs and C276S FHL1 mutants affect contraction parameters in rat EHT

Since hypercontractility and diastolic dysfunction are common features in HCM (22,33), we evaluated whether human FHL1 WT or mutants affect contraction parameters after gene transfer in rat EHT. EHTs were transduced with AAV-6 virus encoding FLAG-FHL1 WT or mutants (Fig. 9). After 14 days,

EHTs were treated with 500 nM of the proteasome inhibitor, epoxomicin, for 24 h, and contraction parameters were measured (Fig. 9). Force and kinetics of contraction did not differ between C153X-, D275N- or WT-transduced EHT (Fig. 9). In contrast, K45Sfs-transduced EHT presented with +27% higher force of contraction, as well as +13% and +30% higher times of contraction (T1) and relaxation (T2) than WT-transduced EHT, respectively. In C276S-transduced EHT, force of contraction was 23% lower, and times of contraction (T1) and relaxation (T2) were 23 and 31% higher than in WT-transduced EHTs, respectively (Fig. 9).

Immunofluorescence analysis of FLAG-FHL1-transduced and epoxomicin-treated EHTs revealed typical alignment of the myocytes, clear striation pattern of cMyBP-C and some striation-like pattern for FHL1 WT, D275N and C276S mutants (Fig. 10). However, the alternation between cMyBP-C and FLAG-FHL1 mutants was not obvious in EHTs. Furthermore, the two truncated mutants K45Sfs and C153X were not well incorporated into the sarcomere and also accumulated in nuclei (Fig. 10).

We finally evaluated whether the expression of *FHL1* gene variants is associated with the re-activation of the fetal gene
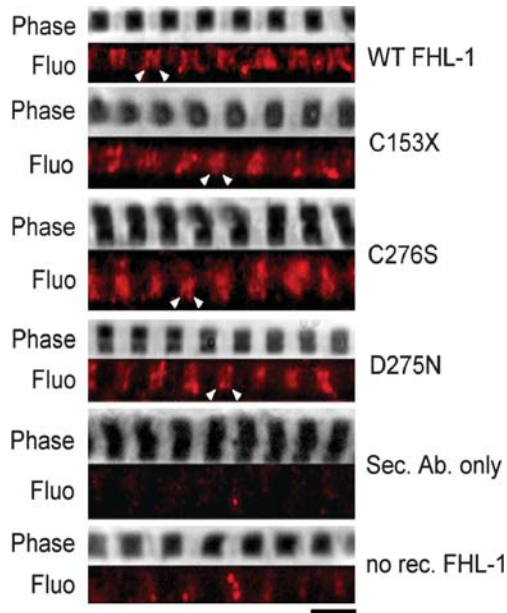
Figure 6. Immunofluorescence images of recombinant FHL1 WT and mutants bound to isolated human cardiac myofibrils. After isolation and stretching, human cardiac myofibrils were incubated with bacterially expressed recombinant FHL1 WT or mutants and then immunostained for FHL1. FHL1 binding to myofibrils resulted in a more or less distinct double-band signal in the I-band region (Cy3-signal in red). Cy3-conjugated secondary antibody alone gave no signal. If no recombinant FHL1 was added prior to antibody staining, no double-band signals were detected. Arrowheads indicate I-band doublet. Fluo, fluorescence image; phase, phase-contrast image; rec., recombinant. Scale bar: 4 μm.

program of hypertrophy. The mRNA levels of rat *Nppa* (atrial natriuretic peptide), *Myh7* (β-myosin heavy chain) and *Acta1* (α-skeletal actin) were higher in EHT transduced with C153X, C276S or D275N mutants than in EHT transduced with WT (Supplementary Material, Fig. S3). Similar results were obtained for *Nppb* (brain natriuretic peptide), except for C276S. In contrast, EHT transduced with the K45Sfs mutant did not activate the fetal hypertrophic gene program.

DISCUSSION

The aim of the present study was to evaluate whether *FHL1* might be a new disease gene for HCM in a cohort of 121 unrelated index cases, who do not carry a mutation in previously identified genes. The major findings are as follows: (i) three novel *FHL1* genetic variants (K45Sfs, C153X and C276S) and two known SNPs (D275N and D147D) were identified in seven unrelated HCM families; (ii) C153X was associated with skeletal muscle weakness in some patients, whereas K45Sfs and C276S were associated with isolated HCM; (iii) FHL1 WT or mutant proteins bound to the I-band of human cardiac myofibrils; (iv) after gene transfer in C2C12 myoblasts or in cardiac myocytes, protein levels of HCM FHL1 mutants were lower than those of WT, but could be rescued by proteasome inhibition; (v) accumulation of mutant aggregates appeared after proteasome inhibition in cardiac myocytes; (vi) force and kinetics of contraction were altered following transduction of EHTs with K45Sfs or C276S mutants and

(vii) most of the mutants activated a fetal gene program of hypertrophy in EHTs. These data provide the first evidence of *FHL1* mutations to be associated with and possibly causative for isolated HCM and of the regulation of their expression at least by the UPS. Our findings suggest that impairment of the UPS with age and/or as a consequence of an initial pathology would lead to aggravation of a toxic effect of FHL1 mutants either by formation of protein aggregates and/or by their effects on sarcomere function. This may result in hypertrophy, hypercontractility or diastolic dysfunction, all common features in human HCM.

Out of the five *FHL1* variants identified in HCM families in the present study, two have been previously recognized as SNPs. The first one is the c.823G>A transition leading to D275N, which has been found in control individuals in a previous study (30) and is reported as an SNP (rs151315725) with an allele frequency of 1.2%. The second one is the c.441C>T transition resulting in D147D, which is reported as an SNP (rs149670651) with a very low allele frequency of 0.2%. This suggests that both polymorphisms are likely not responsible for HCM. This is supported by the following observations. First, and in contrast to the three novel *FHL1* variants (K45Sfs, C153X and C276S), the D275N protein was stable and not degraded by the UPS after transduction of cardiac myocytes (Fig. 7). Secondly, the D275N mutant protein was incorporated into the sarcomere alternating with endogenous cMyBP-C, as observed for FHL1 WT but in contrast to the truncated FHL1 mutants (Figs. 8 and 9). Finally, D275N did not alter the contraction parameters of EHT (Fig. 9). However, the finding that D275N mutant activated a fetal hypertrophic gene program in EHT (Supplementary Material, Fig. S3) suggests that it could cause HCM in these patients. For D147D we did not evaluate its protein level and cellular localization after gene transfer in cardiac myocytes or its effect on EHT contractions, but we predict a behavior similar to WT. However, we cannot exclude a pathogenic role of the D147D variant. Indeed, on the one hand, this is a very rare SNP, and, on the other hand, this c.441C>T transition alters exonic splice enhancer sequences, which regulate the splicing process, and it might therefore produce a truncated protein. Further analyses using minigenes will evaluate this possibility.

Out of the three novel *FHL1* variants (c.134delA/K45Sfs, c.827G>C/C276S and c.459C>A/C153X), K45Sfs and C276S were associated with isolated HCM. Arguments to believe that both variants are causing HCM are as follows. First, *FHL1* has already firmly been established as a disease gene in other inherited muscle diseases (13–17). Secondly, the variants were found in all HCM-affected individuals (Fig. 1 and Table 2). Thirdly, the variants were not found in 285 control individuals. Fourth, the FHL1 mutant proteins resulting from these variants were degraded by the UPS (Figs. 3, 4 and 7 and Supplementary Material, Fig. S2), similar to what has been shown for other HCM sarcomeric mutant proteins previously (34–37). Finally, after proteasome inhibition, K45Sfs and C276S mutants affected contraction parameters of transduced EHTs (Fig. 9). The c.134delA variant is a one-nucleotide deletion, leading to a frameshift (K45Sfs) in the first LIM domain shared by the three FHL1 isoforms and the production of a shorter protein composed
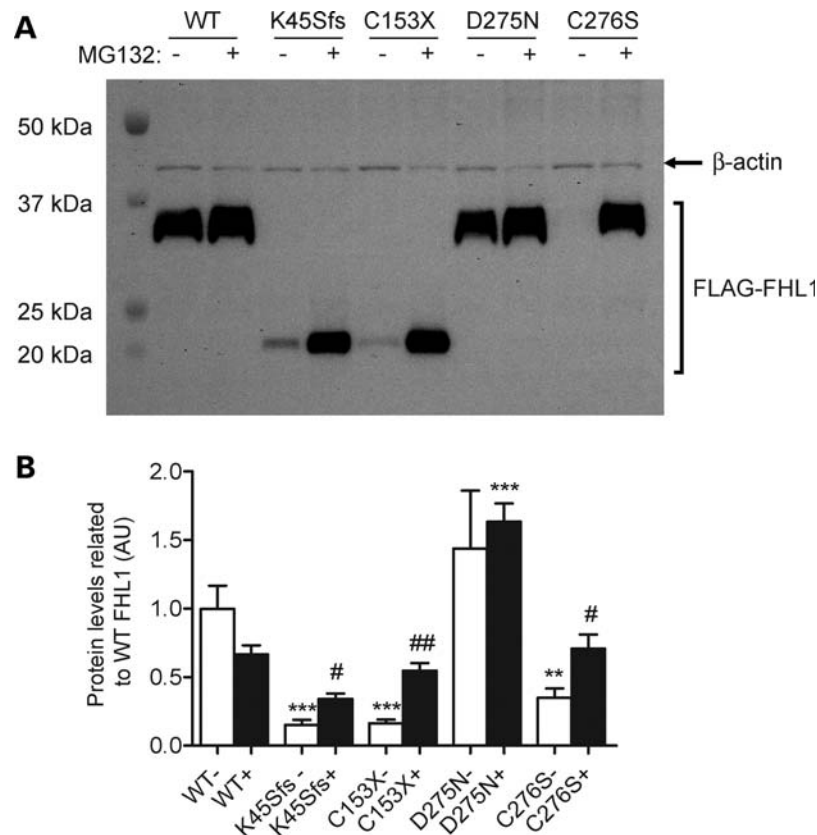
Figure 7. Protein levels of FHL1 WT and mutants after transduction of cardiac myocytes. Cardiac myocytes were isolated from neonatal mice, transduced with AAV serotype 6 (MOI 10 000) encoding FLAG-tagged WT FHL1 or HCM-related mutants for 48 h and then treated (+) or not (−) with 1 μM MG132 for 24 h. (**A**) Representative western blot stained with the FLAG antibody recognizing FLAG-FHL1 WT or mutants and with an antibody directed against β-actin, used as an endogenous control. Molecular weight markers are indicated. (**B**) Protein levels of FLAG-FHL1 mutants, normalized to β-actin levels and indexed to FLAG-FHL1 WT protein levels. Data are expressed as mean ± SEM (*n* = 3–5). **$P < 0.01$ and ***$P < 0.001$ versus WT in the same condition, two-way ANOVA with Bonferroni's multiple comparison test. #$P < 0.05$ and ##$P < 0.01$ versus vehicle, unpaired Student's *t*-test.

of 150 amino acids (Fig. 2). This large truncation of 3.5 LIM domains has never been reported so far (reviewed in 1) and was detected in a hemizygote male index case, who presented with marked septal hypertrophy and outflow tract obstruction, but no skeletal myopathy (Table 1). The resulting K45Sfs mutant protein was markedly unstable in C2C12 myoblasts, COS-1 cells and cardiac myocytes, and could not be expressed in bacteria, suggesting that it may be misfolded and act as a poison peptide. Proteasome inhibition markedly prevented degradation of this mutant protein in different cell types (Figs. 3, 4 and 7 and Supplementary Material, Fig. S2). The K45Sfs mutant also appeared as aggregates in cardiac myocytes (Fig. 8) and induced hypercontractility and prolonged contraction and relaxation in EHTs (Fig. 9). These features may lead to increased LV systolic pressure and diastolic dysfunction, which are common features in human HCM (22). However, this variant did not activate the fetal hypertrophic gene program (Supplementary Material, Fig. S3), probably because it contains less than two LIM domains required for the interaction with MAPK proteins (7). The second *FHL1* variant associated with isolated HCM was the c.827G>C/ C276S, which exhibited features similar to K45Sfs. The resulting C276S mutant protein, despite being full length, was also degraded by the UPS (Fig. 7 and Supplementary Material,

Fig. S2) and induced prolonged contraction and relaxation of EHTs (Fig. 9). However, and in contrast to K45Sfs, it was well incorporated into the sarcomere and did not form aggregates in cardiac myocytes (Fig. 8). In addition, it reduced force of contraction in EHTs (Fig. 9), even at days 9–14 (data not shown), and it induced a fetal hypertrophic gene program (Supplementary Material, Fig. S3). The male index case, hemizygote for the mutation, presented with marked septal hypertrophy. His mother, heterozygote for the mutation, did not exhibit a phenotype, which is compatible with an X-linked transmission. Another mutation that affects the same nucleotide but results in a different amino acid exchange (c.827G>A/C276Y) has been described in an EDMD family, in which the index case also presented with a slight septal hypertrophy, LV dysfunction and unstable FHL1 mutant protein in muscle biopsy (17). Both the C276S and C276Y variants result in loss of a highly conserved cysteine residue within the LIM4 domain, which is present only in the FHL1A isoform, and are suggested to destabilize the zinc-finger structure and thus compromise LIM domain structure and function (38). The last novel *FHL1* variant (c.459C>A/ C153X) was associated with the most striking cardiac phenotype, ranging from borderline to marked septal hypertrophy. The index case underwent heart transplantation at the age of
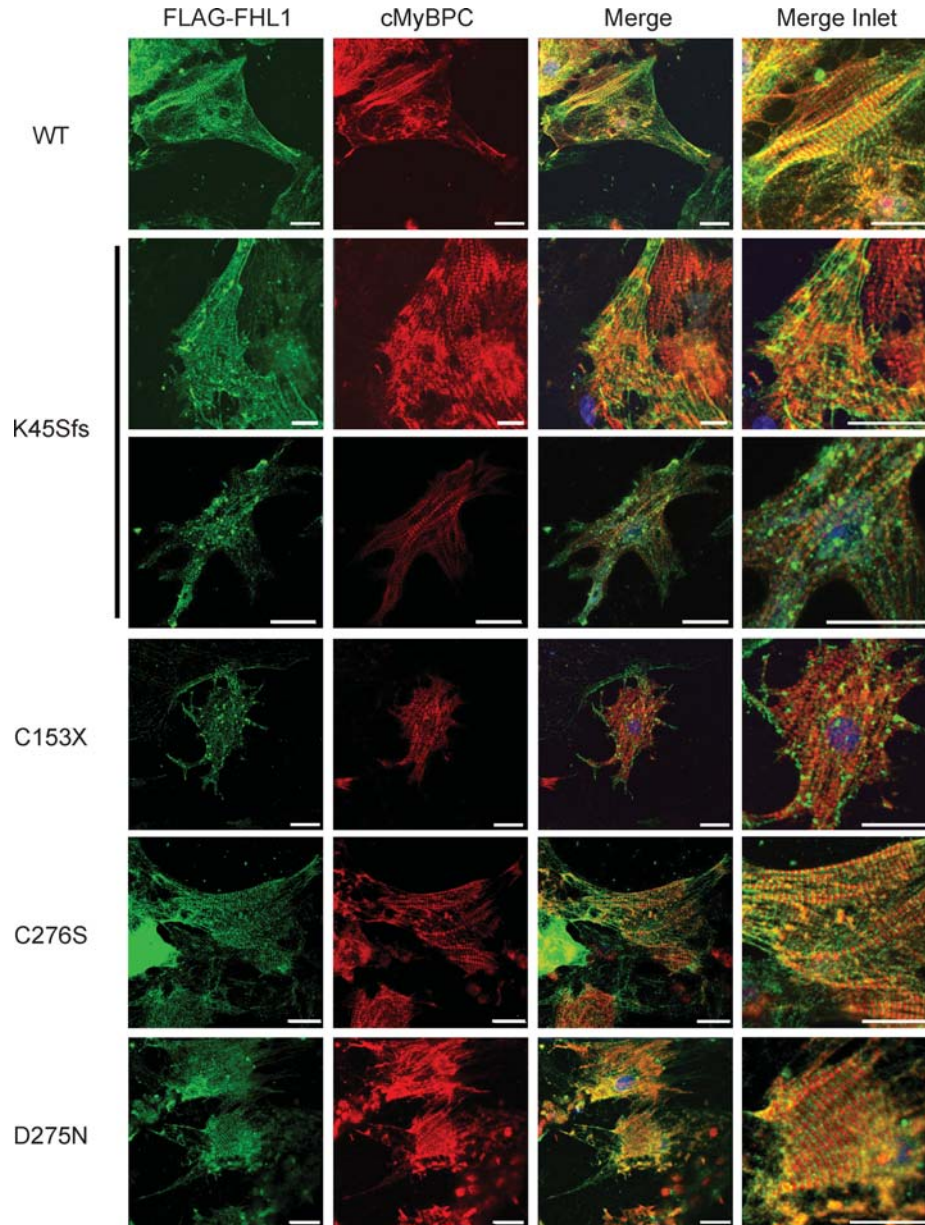
Figure 8. Immunofluorescence images of cardiac myocytes transduced with FHL1 WT or mutants. Cardiac myocytes were isolated from neonatal mice, transduced with AAV serotype 6 (MOI 50 000) encoding FLAG-tagged FHL1 WT or mutants for 48 h and then treated with 1 μM MG132 for 24 h. After fixation, cells were stained with antibodies directed against the FLAG epitope (green) and cMyBP-C (red). Right panels correspond to higher magnifications of merge images. Scale bars: 20 μm.

19. Interestingly, whereas the female affected members, who are heterozygotes for the mutation, developed HCM only, the male affected members, hemizygotes for the mutation, also exhibited muscle defects such as Achilles tendon contractures or diaphragm weakness (Table 2). This variant creates a direct stop codon in the LIM2 domain, yielding a truncated protein consisting of only the N-terminal 2.5 LIM domains, and is therefore likely to have a significant and detrimental effect on FHL1 protein function. As observed for the other 'pure' HCM-associated mutants, C153X mutant protein is markedly unstable in all cell types (Figs. 3, 4 and 7 and Supplementary Material, Fig. S2), and proteasome inhibition prevented its degradation and resulted in aggregates in cardiac myocytes (Fig. 8). In contrast, whereas a trend toward prolonged relaxation (+17%) of the EHTs was observed with C153X, the other contraction parameters were not affected (Fig. 9). While the contractile parameters were not significantly affected, the fetal hypertrophic program was activated with the C153X mutant (Supplementary Material, Fig. S3), suggesting that it may cause HCM without cardiac dysfunction in patients. The C153 amino acid residue has been shown to be mutated in two index cases with RBM (C153Y and C153R), one of these patients also presenting with DCM (39).
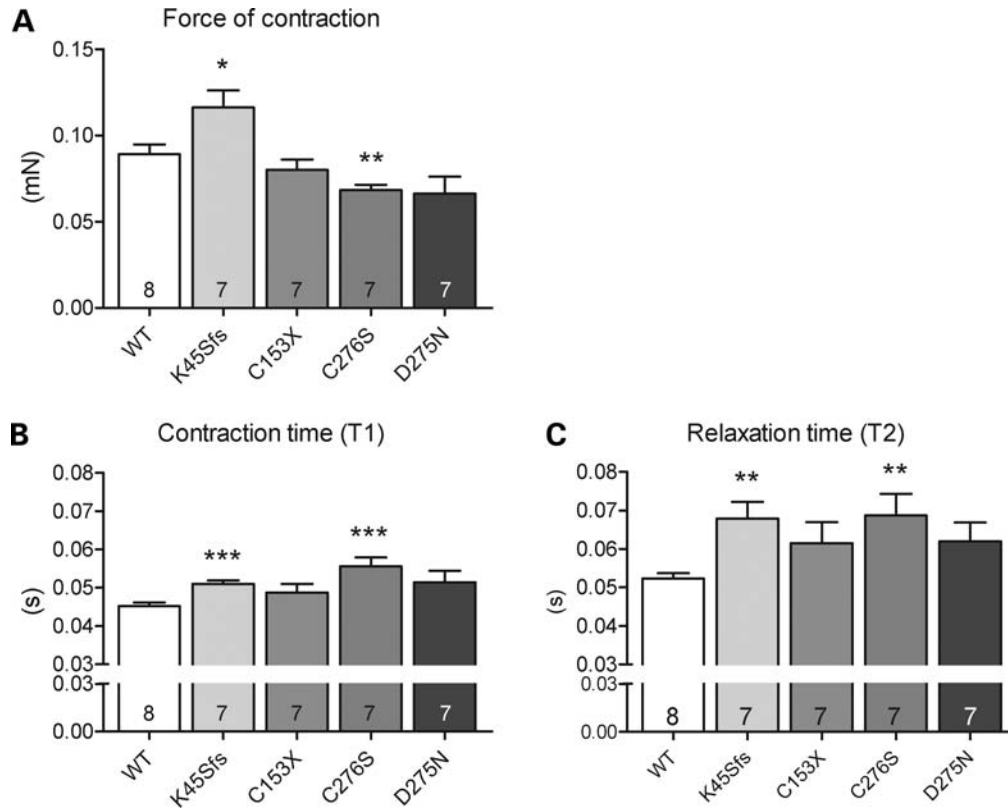
Figure 9. Contractility measurements in EHT transduced with FHL1 WT or mutants. Rat EHTs were transduced at day 0 with AAV serotype 6 (MOI 1000) encoding FLAG-tagged FHL1 WT or mutants and treated at day 14 with 500 nM epoxomicin for 24 h. Force measurements of the EHTs were monitored by video recordings. Data for (**A**) force of contraction, (**B**) contraction time (T1) and (**C**) relaxation time (T2) are shown. Data are expressed as mean ± SEM, with $^*P < 0.05$, $^{**}P < 0.01$ and $^{***}P < 0.001$ versus WT, unpaired Student's t-test. The number of tissues is indicated in the bars.

The precise mechanism by which *FHL1* mutations cause HCM and associated cardiac dysfunction remains elusive. The first hypothesis is a 'loss of normal FHL1 protein function', resulting from deficiency of FHL1 protein and/or loss of critical amino acids required for normal FHL1 protein folding. Our findings provide evidence of marked degradation of HCM-associated FHL1 mutant proteins by the UPS and, to a lower extent, by the autophagy–lysosome pathway (Figs. 3, 4 and 7 and Supplementary Material, Fig. S2). Lower protein levels of mutant FHL1 have also been observed in some of the muscle biopsies of patients with RBM, XMPMA, SPM or EDMD (15,17,30,40), suggesting that proteolytic systems play an important role in preventing formation and accumulation of poison peptides in distinct striated muscle disorders. Although mutant mRNA levels have not been previously determined in muscle biopsies, involvement of the nonsense-mediated mRNA decay as a quality control system, in addition to the proteolytic systems, could not be excluded, as it has been previously demonstrated for other mutations causing HCM, EDMD or long QT syndrome (37,41,42). In male patients, these mutations would lead to a marked deficiency of FHL1 that could in turn impair FHL1 function and/or interaction with FHL1-binding partners. FHL1 interacts with the C10 domain of the sarcomeric protein MyBP-C via the LIM2 domain (8), and FHL1 deficiency could alter the stability of cMyBP-C, which is also mutated in human HCM

(24,43,44). FHL1 has been shown to interact *in vitro* with components of the MAPK pathway and with the N2B domain of titin (7), which is an elastic segment contributing to myofibrillar passive tension (45,46). *Fhl1* deficiency in mice caused a blunted activation of the MAPK pathway and reduced hypertrophic response after transverse aortic constriction, and it also prevented cardiomyopathy in transgenic mice overexpressing Gq (7). The authors proposed that FHL1, together with MAPK components, may be part of a stretch-sensor complex together at the N2B region of titin, and that FHL1 could play a central role in the pathomechanism of hypertrophy by modulating extensibility and MAPK signaling. In our hands, the distinct binding of FHL1 WT protein to the titin N2B domain at the sarcomeric I-band appeared to be compromised with the mutant recombinant constructs. A possibility is that the FHL1 mutant proteins alter the stretch-sensor function at the N2B domain, thus affecting the cardiac hypertrophy response. This is supported by the present findings that all FHL1 mutants except K45Sfs (that could also not be produced in bacteria) activated the fetal gene program of cardiac hypertrophy in EHTs (Supplementary Material, Fig. S3). The absence of the LIM2 domain in K45Sfs and its presence in all the other mutants (Fig. 2) suggest that the LIM2 domain is the minimal requirement for activating the cardiac hypertrophic response. Besides the sarcomere, FHL1 has been found in the nucleus, where it co-activates
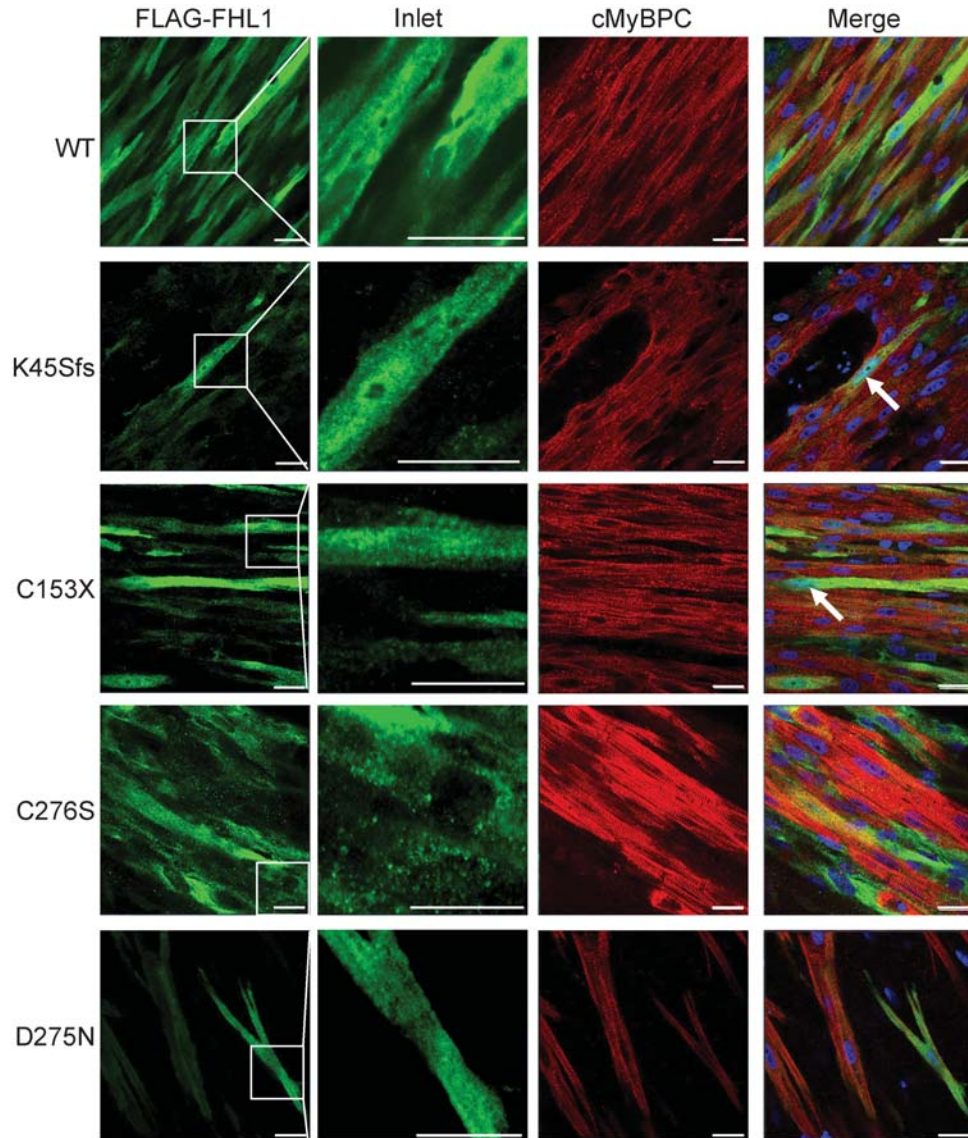
Figure 10. Immunofluorescence images of EHT transduced with FHL1 WT or mutants. Rat EHTs were transduced at day 0 with AAV serotype 6 (MOI 1000) encoding FLAG-tagged FHL1 WT or mutants, treated at day 14 with 500 nM epoxomicin for 24 h and analyzed for contraction parameters. After fixation, tissues were stained with antibodies directed against the FLAG epitope (green) and cMyBP-C (red). Higher magnifications of FLAG-FHL1 images are also shown. White arrows indicate nuclear staining of FLAG-FHL1. Scale bars: 20 μm.

NFATc1-dependent transcription to promote myoblast fusion, muscle hypertrophy and increased muscle strength (reviewed in 1). Impaired ability to undergo myogenesis has been observed in myoblasts from EDMD patients and after gene transfer of different *FHL1* variants in C2C12 myoblasts (17), but could not be investigated in the present study, likely due to the toxic effect of the proteasome on myotube formation. Finally, FHL1 interacts with and regulates the potassium KCNA5 channel in human atrium (9), suggesting that FHL1 deficiency could affect myocardial repolarization. A remaining question is how deficiency of (mutant) FHL1 reconciles with the marked upregulation of *FHL1* expression in human HCM (19,20), in experimental models of cardiac hypertrophy (6,21,47) and in genetically engineered mice with

cardiomyopathy, such as MLP knock-out (6) or *Mybpc3*-targeted knock-out (Supplementary Material, Fig. S4). Whether this is a cause or a consequence of the phenotype in these models remains to be elucidated.

The second hypothesis for the pathogenic effect of *FHL1* mutations is a 'gain of toxic function' through the formation of FHL1 mutant protein aggregates. Intracellular protein aggregates have also been described in RBM, SPM and rigid spine syndrome (14,48). It has been proposed that *FHL1* mutations result in protein misfolding and the exposure of non-polar surfaces, particularly for the mutations that affect the conserved cysteine or histidine residues, which bind zinc and are essential for the stabilization of the LIM domain (49). In RBM, aggregate formation increases with disease

progression (14,48), supporting a toxic gain of function. Interestingly, FHL1-interacting partners such as MyBP-C or NFATc1, α-actinin or desmin, all known to be degraded by the UPS (31), as well as components of the UPS such as ubiquitin, have been shown to be part of the aggregates containing mutant FHL1 proteins (10,14,50). This finding points to an involvement of the UPS in the course of the disease. There is recent evidence that the UPS plays a pathogenic role in HCM and desmin-related cardiomyopathy (31,32,51). Furthermore, we and others recently showed that the UPS is impaired after adrenergic stress in heterozygous asymptomatic *Mybpc3*-targeted knock-in mice (52), with age in homozygous knock-in mice with HCM (53) or in HCM patients (54). This observation supports the hypothesis that stress-induced UPS impairment in HCM could lead to accumulation of FHL1 mutant proteins in aggregates within cardiac myocytes and alteration of the cardiac function, and this may initiate a vicious cycle. The present study also provides experimental evidence that expression of the *FHL1* mutations associated with proteasome inhibition results in accumulation of FHL1 mutant aggregates, activation of the hypertrophic gene program and/or alteration of the contraction parameters in cardiac myocytes or EHTs. Alternatively, protein aggregates may directly inhibit components of the proteasome by 'chocking' the proteases or indirectly interfere with the UPS function by inactivating or depleting UPS components. Disturbed UPS function could result in reduced degradation of other proteins such as the transcription factor NFAT, a known activator of cardiac hypertrophy and FHL1-binding partner, thus promoting maladaptive processes in terms of activation of the hypertrophic gene program (55).

The reason why two *FHL1* mutations are associated with isolated HCM without skeletal muscle manifestations is not certain, but the hypothesis of cardiac-specific UPS impairment is supported by the following findings. First, the marked reduction in the level of FHL1 mutant proteins is a common and specific feature in patients presenting with HCM, EDMD or XMPMA (13,17,30). Secondly, HCM is a common phenotype in patients presenting with EDMD or XMPMA (13,17), and the cardiac phenotype is sometimes the only clinical manifestation in EDMD male patients (17). Thirdly, some index cases with EDMD or XMPMA have a late onset of skeletal muscle manifestations (17,30). Fourth, no evidence of UPS impairment has been described in skeletal muscle of patients with EDMD or XMPMA; in contrast, a series of evidence indicate UPS impairment in myocardial tissue of HCM patients and mouse models (52–54). Therefore, we believe that the expression of *FHL1* mutations associated with cardiac-specific UPS impairment may lead to isolated HCM.

In conclusion, this study provides evidence for *FHL1* as a novel disease gene for isolated HCM without associated myopathy. These findings add further complexity to our understanding of the pathogenic effect of *FHL1* mutations. Our data, together with previous findings of proteasome impairment in HCM, suggest that FHL1 mutants may accumulate and act as poison peptides, leading to hypertrophy, diastolic dysfunction and/or altered contractility, which are features of HCM. Screening of *FHL1* for mutations should be systematically considered for HCM patients with yet unidentified mutations.

MATERIALS AND METHODS

Patients

We enrolled 121 HCM index cases who do not carry a mutation in *MYH7*, *MYBPC3*, *TNNT2* (encoding cardiac troponin T), *TNNI3* (encoding cardiac troponin I) or *MYL2* (encoding regulatory myosin light chain; data not shown). They were selected out of 299 HCM index cases recruited from the Eurogene Heart Failure cohort supported by the Leducq Foundation (56). Patients were diagnosed based on medical history, physical examination, ECG and echocardiogram (LV wall thickness ≥15 mm in probands and >13 mm in relatives) (57). Controls consisted of 285 individuals. All materials from patients and controls were taken with the informed consent of the donors and with approval of the local ethical boards.

Mutation screening of *FHL1*

The *FHL1* gene has eight exons, of which five (exons 3–6 and exon 8) code for the isoform FHL1A, six (exons 3–8) for FHL1B and four (exons 3–5 and exon 8) for FHL1C. The isoform primarily expressed in heart is FHL1A (3). Therefore, only the five coding exons for FHL1A, including neighboring intron boundaries, were screened by polymerase chain reaction (PCR) amplification performed on 30 ng of genomic DNA from peripheral lymphocytes using primer pairs (Supplementary Material, Table S1). Sequences were examined by using Codon Code Aligner Software®. Reference *FHL1* sequence was taken from NCBI (NC_000023.10) with +1 designing the A of ATG codon.

Plasmid constructs

The pCGN-FHL1A plasmid containing human *FHL1A* cDNA (GenBank accession no. NM_001449), pCGN-FHL1A RBM^{C132F} mutant and pCGN-βgal (vector control) have been described previously (10). The following mutants, described previously, were used for comparison: c.266G>C (SPM^{W122S}; 49), c.C381_382insATC (XMPMA$^{127–128insI}$; 13), c.672C>G (C224W; 30), c.827G>A (EDMD^{C276Y}; 17), c.del304-312AAGGGGTGC (RBM$^{102–104delKFC}$; 40) and c.del451–459GTGACTTGC (RBM$^{151–153delVTC}$; 15). Mutations identified in the present study were introduced into WT FHL1A via PCR mutagenesis (primers are given in Supplementary Material, Table S2) and ligated into PCR-Blunt: c.134delA/K45Sfs, c.459C>A/C153X, c.827G>C/C276S and c.823G>A/D275N. All variants contained an HA-tagged sequence after the ATG. For C2C12 myoblast experiments, the *FHL1A* cDNA variants were directionally cloned into pCGN with 5′ *Xba*I and 3′ *Sma*I restriction sites. For recombinant proteins and production of AAV-6, the different *FHL1A* cDNA variants were subcloned using the pEF5/FRT/V5-D-TOPO expression kit (Invitrogen, Life Technology, Darmstadt, Germany) and the pCGN/PCR-Blunt vectors as template with primers containing specific restriction sites to allow insertion into the cloning vector (Supplementary Material, Table S3).

Production of recombinant proteins

The different *FHL1A* cDNA variants were cloned into the pGEX-5X-1 vector and used to transform BL21 bacteria. After culture, the proteins were harvested and purified using the Glutathione S-Transferase Gene Fusion System (GE Healthcare, Munich, Germany), as described previously (37).

Production of AAV

Two FLAG tags were inserted after the ATG of WT and mutant FHL1 constructs by PCR. The FLAG-tagged variants were subcloned into the pdsAAV-CMV-MLC260 vector under control of the CMV-enhanced myosin light chain-2v promoter for AAV-6 production, as described previously (58). AAV-6 titers ranged from 5.76 to 9.66×10^{11} virus genomes per ml (Vg/ml).

C2C12 myoblasts culture, transfection, western blot and immunofluorescence analyses

C2C12 myoblasts (American Type Culture Collection) were grown and transfected, as described previously (10). Briefly, C2C12 myoblasts were passaged at subconfluency in growth medium [GM; 20% fetal calf serum (FCS), 2 mM L-glutamine], supplemented with penicillin/streptomycin (P/S) before seeding into six-well plates in P/S-free GM [2×10^5 cells/well; fibronectin-coated cover slips (5 µg/ml) for microscopy]. After 24 h, cells were transfected with 1−4 µg of plasmid cDNA and 2−8 µl of Lipofectamine 2000 (Invitrogen) in 1 ml of Optimem (Invitrogen, Life Technology, Darmstadt, Germany) for 4 h before returning to P/S-free GM. After 24 h, cells were treated for 24 h with 20 µM MG132 in 0.1% DMSO, 5 nM bafilomycin-A1 in 0.1% DMSO or with vehicle alone (all from Sigma-Aldrich Chemie Gmbh, Munich, Germany).

For western blot analysis, scraped myoblasts were harvested in 1% Triton X-100 with protease inhibitors (Merck, Darmstadt, Germany) in Tris saline solution for 1 h rocking before centrifugation at 10 000g for 10 min. The soluble lysates were denatured with reducing buffer by heating to 95°C for 5 min before sodium dodecyl sulfate−polyacrylamide gel electrophoresis analysis. Membranes were incubated with primary antibodies diluted in blocking solution [mouse anti-HA (Covance, Princeton, New Jersey, USA) and β-tubulin (Invitrogen, Life Technology, Darmstadt, Germany), both 1:1000], followed by horseradish peroxidase (HRP)-conjugated anti-mouse antibody (GE Healthcare Life Sciences, Munich, Germany; 1:600). Densitometry was performed in ImageJ and statistical analysis in LibreOffice Calc. Band intensities were normalized to β-tubulin loading.

For immunofluorescence, treated cells were fixed and permeabilized [4% formaldehyde and 0.1% Triton X-100 in phosphate-buffered saline (PBS)], blocked [1% bovine serum albumin (BSA)] and incubated with mouse anti-HA antibody (Covance, Munich, Germany, 1:1000) diluted in blocking solution followed by Alexa-fluor 488-conjugated secondary antibody (Invitrogen, 1:600) and 4'-6-diamidino-2-phenylindole (DAPI) nuclear stain (8). Microscopy was performed at

Monash Microimaging, Monash University, Australia. Samples for microscopy were mounted in Fluoromount-G (Southern Biotech, Birmingham, AL, USA) or SlowFade reagent (Invitrogen, Life Technology, Darmstadt, Germany) and viewed at room temperature. Confocal microscopy was performed using an upright confocal laser scanning microscope (Nikon C1). For quantification, myoblasts were scored as HA-positive if their fluorescence intensity was significantly above background staining (thresholded in ImageJ). The number of HA-positive cells was expressed as a percentage relative to the number of FHL1-WT-transfected cells.

Mechanical manipulation and fluorescence staining of isolated human myofibrils

Myofibrils were isolated from LVs of human donor hearts and prepared for mechanical measurements, as described previously (59). Isolated myofibrils were stretched and incubated with recombinant FHL1 protein (WT or mutants) at a concentration of ∼1.0 µg/µl relaxing buffer. After washout of unbound protein, anti-FHL1 antibody (Abcam no. 76912, 1:50) followed by Cy3-conjugated secondary antibody (Invitrogen, Life Technology, Darmstadt, Germany, 1:500) was added to the buffer. After washout, bound FHL1 was visualized under a Zeiss Axiovert 135 microscope in epifluorescence mode (100× objective) using a CCD camera (Andor iXon; Andor Belfast, Northern Ireland, UK) and Andor software. Exposure time usually was 1 s.

Cardiac myocytes culture, transduction, western blot and immunofluorescence analyses

Cardiac myocytes were isolated from newborn (NMCMs) or adult (AMVMs) C57/BL6J mice, as described previously (37,60). NMCMs were plated at a density of 330 000 cells/well in 12-well plates. NMCMs were transduced with AAV-6 encoding the respective variants at an MOI of 10 000−50 000 on day 0 of culture. When indicated, cells were treated with 1 µM MG132, an established proteasome inhibitor, for 24 h.

For western blot analysis, NMCMs were harvested 72 h after culture, proteins were extracted and western blots performed, as described previously (37). Membranes were stained with a monoclonal antibody directed against the FLAG epitope (Sigma-Aldrich Chemie Gmbh, Munich, Germany, 1:5000) and β-actin (Sigma-Aldrich Chemie Gmbh, Munich, Germany). The secondary antibody was coupled to HRP (POX, Dianova, Hamburg, Germany). Signal was detected by ECL Plus western blotting detection system substrate (Amersham GE Healthcare Life Sciences, Munich, Germany). Quantification of the signal was determined using Genetools software (Syngene, Cambridge, UK).

For immunofluorescence analysis, NMCMs or AMVMs were plated on glass cover slips and processed, as described previously (36,37,60). Cells were incubated with primary antibodies against FHL1 (Abcam, Cambridge, UK, no. 76912, 1:250), FLAG (Abcam, Cambridge, UK, 1:800), cMyBPC (either directed against the C0 domain, custom antibody, dilution 1:200 or directed against the first 14 amino acids, dilution

1:10 000 (61)] and α-actinin (Sigma-Aldrich Chemie Gmbh, Munich, Germany, 1:200). Secondary antibody staining was done with Alexa-fluor 488 anti-mouse and Alexa-fluor 546 anti-rabbit (both Invitrogen, Life Technology, Darmstadt, Germany, 1:600). Nuclei were stained with Topro (1:1000). Signals were visualized with a Carl Zeiss confocal microscope (Zeiss LSM 510 META). Confocal images were recorded using a Zeiss LSM 5 Image system.

EHT generation, transduction, immunofluorescence and contraction measurements

Generation of EHT from neonatal rat heart cells was performed, as described previously (62). Briefly, a reconstitution mix ($n = 16$ for each *FHL1* variant) containing 5×10^5 cells/EHT, bovine fibrinogen, aprotinin and Dulbecco's modified Eagle's medium (DMEM) (including 1% P/S, 1% L-glutamine and 10% FCS) was prepared on ice. After preparation of the casting molds in 24-well plates by agarose solidification, silicon post racks were placed into the dishes with pairs of posts reaching into each casting mold. For each EHT, a 100 µl reconstitution mix was mixed quickly with 3 µl thrombin and added into the agarose slot. After 2 h of incubation at 37°C, 7% CO_2, the racks were transferred to new 24-well plates with 1.5 ml fresh EHT medium.

EHTs were transduced with AAV-6 encoding FHL1 WT or mutants (K45Sfs, C153X, C276S and D275N) at an MOI of 1000. The transduction was performed directly in the reconstitution mix before pipetting it into the agarose slots. To maintain the isotonic conditions, $2\times$ DMEM was added matching the virus volume. Constructs were then cultured at 37°C in a 7% CO_2-humidified cell culture incubator for 15 days. At day 14, the EHTs were treated for 24 h with 500 nM epoxomicin (in 0.1% DMSO), a selective proteasome inhibitor.

Contraction measurements were performed on days 7, 9, 12, 14 and 15, as described previously (62,63). Briefly, contractions of EHTs were monitored by video recording. Recorded contractions were identified by peak criteria. Analysis of the recording was performed using a customized software (www.ctmv.de), based on figure recognition of the contracting muscle strip in a fully automated manner. Values for average force, contraction time (T1) and relaxation time (T2) were calculated, depending on the recognized contractions.

For immunofluorescence analysis, the entire EHTs were analyzed using confocal imaging. EHTs were rinsed with PBS and fixed with Histofix® (Carl Roth GmbH, Karlsruhe, Germany) overnight at 4°C. The samples were then removed from the silicon post and treated for 24 h with blocking solution (Tris-buffered saline 0.05 M, pH 7.4, 10% FCS, 1% BSA, 0.5% Triton X-100) at 4°C. Immunofluorescence was performed as described earlier (primary antibodies against FLAG (Abcam, Cambridge, UK, 1:800), and cMyBPC, (custom 1:200)). Primary and secondary antibodies were each incubated for 24 h. Finally, the EHTs were fixed between a cover slip and a glass slide, and the fluorescence signal was analyzed using a Carl Zeiss confocal microscope (Zeiss LSM 510 META). Confocal images were recorded with a Zeiss LSM 5 Image system.

Statistical analysis

Data are presented as mean $\pm$ SEM. Statistical analyses were performed using the unpaired Student's *t*-test or the two-way analysis of variance (ANOVA) with Bonferroni's multiple comparison test, as indicated in the legends of figures using the GraphPad software (GraphPad Software Inc., San Diego, CA, USA). A value of $P < 0.05$ was considered significant.

SUPPLEMENTARY MATERIAL

Supplementary Material is available at *HMG* online.

REFERENCES

1. Cowling, B.S., Cottle, D.L., Wilding, B.R., D'Arcy, C.E., Mitchell, C.A. and McGrath, M.J. (2011) Four and a half LIM protein 1 gene mutations cause four distinct human myopathies: a comprehensive review of the clinical, histological and pathological features. *Neuromuscul. Disord.*, **21**, 237–251.
2. Bach, I. (2000) The LIM domain: regulation by association. *Mech. Dev.*, **91**, 5–17.
3. Brown, S., McGrath, M.J., Ooms, L.M., Gurung, R., Maimone, M.M. and Mitchell, C.A. (1999) Characterization of two isoforms of the skeletal muscle LIM protein 1, SLIM1. Localization of SLIM1 at focal adhesions and the isoform slimmer in the nucleus of myoblasts and cytoplasm of myotubes suggests distinct roles in the cytoskeleton and in nuclear-cytoplasmic communication. *J. Biol. Chem.*, **274**, 27083–27091.
4. Robinson, P.A., Brown, S., McGrath, M.J., Coghill, I.D., Gurung, R. and Mitchell, C.A. (2003) Skeletal muscle LIM protein 1 regulates integrin-mediated myoblast adhesion, spreading, and migration. *Am. J. Physiol. Cell Physiol.*, **284**, C681–C695.
5. Muller, J.M., Metzger, E., Greschik, H., Bosserhoff, A.K., Mercep, L., Buettner, R. and Schule, R. (2002) The transcriptional coactivator FHL2 transmits Rho signals from the cell membrane into the nucleus. *EMBO J.*, **21**, 736–748.

6. Chu, P.H., Ruiz-Lozano, P., Zhou, Q., Cai, C. and Chen, J. (2000) Expression patterns of FHL/SLIM family members suggest important functional roles in skeletal muscle and cardiovascular system. *Mech. Dev.*, **95**, 259–265.

7. Sheikh, F., Raskin, A., Chu, P.H., Lange, S., Domenighetti, A.A., Zheng, M., Liang, X., Zhang, T., Yajima, T., Gu, Y. *et al.* (2008) An FHL1-containing complex within the cardiomyocyte sarcomere mediates hypertrophic biomechanical stress responses in mice. *J. Clin. Invest.*, **118**, 3870–3880.

8. McGrath, M.J., Cottle, D.L., Nguyen, M.A., Dyson, J.M., Coghill, I.D., Robinson, P.A., Holdsworth, M., Cowling, B.S., Hardeman, E.C., Mitchell, C.A. *et al.* (2006) Four and a half LIM protein 1 binds myosin-binding protein C and regulates myosin filament formation and sarcomere assembly. *J. Biol. Chem.*, **281**, 7666–7683.

9. Yang, Z., Browning, C.F., Hallaq, H., Yermalitskaya, L., Esker, J., Hall, M.R., Link, A.J., Ham, A.J., McGrath, M.J., Mitchell, C.A. *et al.* (2008) Four and a half LIM protein 1: a partner for KCNA5 in human atrium. *Cardiovasc. Res.*, **78**, 449–457.

10. Cowling, B.S., McGrath, M.J., Nguyen, M.A., Cottle, D.L., Kee, A.J., Brown, S., Schessl, J., Zou, Y., Joya, J., Bonnemann, C.G. *et al.* (2008) Identification of FHL1 as a regulator of skeletal muscle mass: implications for human myopathy. *J. Cell Biol.*, **183**, 1033–1048.

11. Taniguchi, Y., Furukawa, T., Tun, T., Han, H. and Honjo, T. (1998) LIM protein KyoT2 negatively regulates transcription by association with the RBP-J DNA-binding protein. *Mol. Cell. Biol.*, **18**, 644–654.

12. Ng, E.K., Lee, S.M., Li, H.Y., Ngai, S.M., Tsui, S.K., Waye, M.M., Lee, C.Y. and Fung, K.P. (2001) Characterization of tissue-specific LIM domain protein (FHL1C) which is an alternatively spliced isoform of a human LIM-only protein (FHL1). *J. Cell. Biochem.*, **82**, 1–10.

13. Windpassinger, C., Schoser, B., Straub, V., Hochmeister, S., Noor, A., Lohberger, B., Farra, N., Petek, E., Schwarzbraun, T., Ofner, L. *et al.* (2008) An X-linked myopathy with postural muscle atrophy and generalized hypertrophy, termed XMPMA, is caused by mutations in FHL1. *Am. J. Hum. Genet.*, **82**, 88–99.

14. Schessl, J., Zou, Y., McGrath, M.J., Cowling, B.S., Maiti, B., Chin, S.S., Sewry, C., Battini, R., Hu, Y., Cottle, D.L. *et al.* (2008) Proteomic identification of FHL1 as the protein mutated in human reducing body myopathy. *J. Clin. Invest.*, **118**, 904–912.

15. Shalaby, S., Hayashi, Y.K., Goto, K., Ogawa, M., Nonaka, I., Noguchi, S. and Nishino, I. (2008) Rigid spine syndrome caused by a novel mutation in four-and-a-half LIM domain 1 gene (FHL1). *Neuromuscul. Disord.*, **18**, 959–961.

16. Quinzii, C.M., Vu, T.H., Min, K.C., Tanji, K., Barral, S., Grewal, R.P., Kattah, A., Camano, P., Otaegui, D., Kunimatsu, T. *et al.* (2008) X-linked dominant scapuloperoneal myopathy is due to a mutation in the gene encoding four-and-a-half-LIM protein 1. *Am. J. Hum. Genet.*, **82**, 208–213.

17. Gueneau, L., Bertrand, A.T., Jais, J.P., Salih, M.A., Stojkovic, T., Wehnert, M., Hoeltzenbein, M., Spuler, S., Saitoh, S., Verschueren, A. *et al.* (2009) Mutations of the FHL1 gene cause Emery–Dreifuss muscular dystrophy. *Am. J. Hum. Genet.*, **85**, 338–353.

18. Knoblauch, H., Geier, C., Adams, S., Budde, B., Rudolph, A., Zacharias, U., Schulz-Menger, J., Spuler, A., Yaou, R.B., Nurnberg, P. *et al.* (2010) Contractures and hypertrophic cardiomyopathy in a novel FHL1 mutation. *Ann. Neurol.*, **67**, 136–140.

19. Hwang, D.M., Dempsey, A.A., Wang, R.X., Rezvani, M., Barrans, J.D., Dai, K.S., Wang, H.Y., Ma, H., Cukerman, E., Liu, Y.Q. *et al.* (1997) A genome-based resource for molecular cardiovascular medicine: toward a compendium of cardiovascular genes. *Circulation*, **96**, 4146–4203.

20. Lim, D.S., Roberts, R. and Marian, A.J. (2001) Expression profiling of cardiac genes in human hypertrophic cardiomyopathy: insight into the pathogenesis of phenotypes. *J. Am. Coll. Cardiol.*, **38**, 1175–1180.

21. Gaussin, V., Tomlinson, J.E., Depre, C., Engelhardt, S., Antos, C.L., Takagi, G., Hein, L., Topper, J.N., Liggett, S.B., Olson, E.N. *et al.* (2003) Common genomic response in different mouse models of beta-adrenergic-induced cardiomyopathy. *Circulation*, **108**, 2926–2933.

22. Gersh, B.J., Maron, B.J., Bonow, R.O., Dearani, J.A., Fifer, M.A., Link, M.S., Naidu, S.S., Nishimura, R.A., Ommen, S.R., Rakowski, H. *et al.* (2011) 2011 ACCF/AHA guideline for the diagnosis and treatment of hypertrophic cardiomyopathy: a report of the American College of Cardiology Foundation/American Heart Association Task Force on Practice Guidelines. *J. Thorac. Cardiovasc. Surg.*, **142**, e153–e203.

23. Elliott, P., Andersson, B., Arbustini, E., Bilinska, Z., Cecchi, F., Charron, P., Dubourg, O., Kuhl, U., Maisch, B., McKenna, W.J. *et al.* (2008) Classification of the cardiomyopathies: a position statement from the European Society of Cardiology Working Group on Myocardial and Pericardial Diseases. *Eur. Heart J.*, **29**, 270–276.

24. Schlossarek, S., Mearini, G. and Carrier, L. (2011) Cardiac myosin-binding protein C in hypertrophic cardiomyopathy: mechanisms and therapeutic opportunities. *J. Mol. Cell. Cardiol.*, **50**, 613–620.

25. Seidman, C. (2002) Genetic causes of inherited cardiac hypertrophy: Robert L. Frye Lecture. *Mayo Clin. Proc.*, **77**, 1315–1319.

26. Richard, P., Villard, E., Charron, P. and Isnard, R. (2006) The genetic bases of cardiomyopathies. *J. Am. Coll. Cardiol.*, **48**, A79–A89.

27. Friedrich, F.W. and Carrier, L. (2012) Genetics of hypertrophic and dilated cardiomyopathy. *Curr. Pharm. Biotechnol.* [Epub ahead of print].

28. Dougu, N., Joho, S., Shan, L., Shida, T., Matsuki, A., Uese, K., Hirono, K., Ichida, F., Tanaka, K., Nishino, I. *et al.* (2009) Novel LAMP-2 mutation in a family with Danon disease presenting with hypertrophic cardiomyopathy. *Circ. J.*, **73**, 376–380.

29. Yang, Z., McMahon, C.J., Smith, L.R., Bersola, J., Adesina, A.M., Breinholt, J.P., Kearney, D.L., Dreyer, W.J., Denfield, S.W., Price, J.F. *et al.* (2005) Danon disease as an underrecognized cause of hypertrophic cardiomyopathy in children. *Circulation*, **112**, 1612–1617.

30. Schoser, B., Goebel, H.H., Janisch, I., Quasthoff, S., Rother, J., Bergmann, M., Muller-Felber, W. and Windpassinger, C. (2009) Consequences of mutations within the C terminus of the FHL1 gene. *Neurology*, **73**, 543–551.

31. Mearini, G., Schlossarek, S., Willis, M.S. and Carrier, L. (2008) The ubiquitin–proteasome system in cardiac dysfunction. *Biochim. Biophys. Acta*, **1782**, 749–763.

32. Schlossarek, S. and Carrier, L. (2011) The ubiquitin–proteasome system in cardiomyopathies. *Curr. Opin. Cardiol.*, **26**, 190–195.

33. Ferrans, V.J. and Rodriguez, E.R. (1983) Specificity of light and electron microscopic features of hypertrophic obstructive and nonobstructive cardiomyopathy. Qualitative, quantitative and etiologic aspects. *Eur. Heart J.*, **4** (Suppl. F), 9–22.

34. Bahrudin, U., Morisaki, H., Morisaki, T., Ninomiya, H., Higaki, K., Nanba, E., Igawa, O., Takashima, S., Mizuta, E., Miake, J. *et al.* (2008) Ubiquitin–proteasome system impairment caused by a missense cardiac myosin-binding protein C mutation and associated with cardiac dysfunction in hypertrophic cardiomyopathy. *J. Mol. Biol.*, **384**, 896–907.

35. Sarikas, A., Carrier, L., Schenke, C., Doll, D., Flavigny, J., Lindenberg, K.S., Eschenhagen, T. and Zolk, O. (2005) Impairment of the ubiquitin–proteasome system by truncated cardiac myosin binding protein C mutants. *Cardiovasc. Res.*, **66**, 33–44.

36. Mearini, G., Gedicke, C., Schlossarek, S., Witt, C.C., Kramer, E., Cao, P., Gomes, M.D., Lecker, S.H., Labeit, S., Willis, M.S. *et al.* (2010) Atrogin-1 and MuRF1 regulate cardiac MyBP-C levels via different mechanisms. *Cardiovasc. Res.*, **85**, 357–366.

37. Vignier, N., Schlossarek, S., Fraysse, B., Mearini, G., Kramer, E., Pointu, H., Mougenot, N., Guiard, J., Reimer, R., Hohenberg, H. *et al.* (2009) Nonsense-mediated mRNA decay and ubiquitin–proteasome system regulate cardiac myosin-binding protein C mutant levels in cardiomyopathic mice. *Circ. Res.*, **105**, 239–248.

38. Michelsen, J.W., Sewell, A.K., Louis, H.A., Olsen, J.I., Davis, D.R., Winge, D.R. and Beckerle, M.C. (1994) Mutational analysis of the metal sites in an LIM domain. *J. Biol. Chem.*, **269**, 11108–11113.

39. Schessl, J., Columbus, A., Hu, Y., Zou, Y., Voit, T., Goebel, H.H. and Bonnemann, C.G. (2010) Familial reducing body myopathy with cytoplasmic bodies and rigid spine revisited: identification of a second LIM domain mutation in FHL1. *Neuropediatrics*, **41**, 43–46.

40. Shalaby, S., Hayashi, Y.K., Nonaka, I., Noguchi, S. and Nishino, I. (2009) Novel FHL1 mutations in fatal and benign reducing body myopathy. *Neurology*, **72**, 375–376.

41. Muchir, A., Massart, C., van Engelen, B.G., Lammens, M., Bonne, G. and Worman, H.J. (2006) Proteasome-mediated degradation of integral inner nuclear membrane protein emerin in fibroblasts lacking A-type lamins. *Biochem. Biophys. Res. Commun.*, **351**, 1011–1017.

42. Gong, Q., Zhang, L., Vincent, G.M., Horne, B.D. and Zhou, Z. (2007) Nonsense mutations in hERG cause a decrease in mutant mRNA transcripts by nonsense-mediated mRNA decay in human long-QT syndrome. *Circulation*, **116**, 17–24.

43. van Dijk, S.J., Dooijes, D., Dos Remedios, C., Michels, M., Lamers, J.M., Winegrad, S., Schlossarek, S., Carrier, L., Ten Cate, F.J., Stienen, G.J.

et al. (2009) Cardiac myosin-binding protein C mutations and hypertrophic cardiomyopathy. Haploinsufficiency, deranged phosphorylation, and cardiomyocyte dysfunction. *Circulation*, **119**, 1473–1483.

44. van Dijk, S.J., Paalberends, E.R., Najafi, A., Michels, M., Sadayappan, S., Carrier, L., Boontje, N.M., Kuster, D.W., van Slegtenhorst, M., Dooijes, D. *et al.* (2012) Contractile dysfunction irrespective of the mutant protein in human hypertrophic cardiomyopathy with normal systolic function. *Circ. Heart Fail.*, **5**, 36–46.

45. Linke, W.A., Rudy, D.E., Centner, T., Gautel, M., Witt, C., Labeit, S. and Gregorio, C.C. (1999) I-band titin in cardiac muscles is a three-element molecular spring and is critical for maintaining thin filament structure. *J. Cell Biol.*, **146**, 631–644.

46. LeWinter, M.M., Wu, Y., Labeit, S. and Granzier, H. (2007) Cardiac titin: structure, functions and role in disease. *Clin. Chim. Acta*, **375**, 1–9.

47. Kwapiszewska, G., Wygrecka, M., Marsh, L.M., Schmitt, S., Trosser, R., Wilhelm, J., Helmus, K., Eul, B., Zakrzewicz, A., Ghofrani, H.A. *et al.* (2008) Fhl-1, a new key protein in pulmonary hypertension. *Circulation*, **118**, 1183–1194.

48. Schessl, J., Taratuto, A.L., Sewry, C., Battini, R., Chin, S.S., Maiti, B., Dubrovsky, A.L., Erro, M.G., Espada, G., Robertella, M. *et al.* (2009) Clinical, histological and genetic characterization of reducing body myopathy caused by mutations in FHL1. *Brain*, **132**, 452–464.

49. Chen, D.H., Raskind, W.H., Parson, W.W., Sonnen, J.A., Vu, T., Zheng, Y., Matsushita, M., Wolff, J., Lipe, H. and Bird, T.D. (2010) A novel mutation in FHL1 in a family with X-linked scapuloperoneal myopathy: phenotypic spectrum and structural study of FHL1 mutations. *J. Neurol. Sci.*, **296**, 22–29.

50. Liewluck, T., Hayashi, Y.K., Ohsawa, M., Kurokawa, R., Fujita, M., Noguchi, S., Nonaka, I. and Nishino, I. (2007) Unfolded protein response and aggresome formation in hereditary reducing-body myopathy. *Muscle Nerve*, **35**, 322–326.

51. Su, H. and Wang, X. (2010) The ubiquitin–proteasome system in cardiac proteinopathy: a quality control perspective. *Cardiovasc. Res.*, **85**, 253–262.

52. Schlossarek, S., Schuermann, F., Geertz, B., Mearini, G., Eschenhagen, T. and Carrier, L. (2011) Adrenergic stress reveals septal hypertrophy and proteasome impairment in heterozygous Mybpc3-targeted knock-in mice. *J. Muscle Res. Cell Motil.*. [Epub ahead of print].

53. Schlossarek, S., Englmann, D.R., Sultan, K.R., Sauer, M., Eschenhagen, T. and Carrier, L. (2012) Defective proteolytic systems in Mybpc3-targeted mice with cardiac hypertrophy. *Basic Res. Cardiol.*, **107**, 1–13.

54. Predmore, J.M., Wang, P., Davis, F., Bartolone, S., Westfall, M.V., Dyke, D.B., Pagani, F., Powell, S.R. and Day, S.M. (2010) Ubiquitin proteasome dysfunction in human hypertrophic and dilated cardiomyopathies. *Circulation*, **121**, 997–1004.

55. Tang, M., Li, J., Huang, W., Su, H., Liang, Q., Tian, Z., Horak, K.M., Molkentin, J.D. and Wang, X. (2010) Proteasome functional insufficiency activates the calcineurin–NFAT pathway in cardiomyocytes and promotes maladaptive remodelling of stressed mouse hearts. *Cardiovasc. Res.*, **88**, 424–433.

56. Friedrich, F.W., Bausero, P., Sun, Y., Treszl, A., Kramer, E., Juhr, D., Richard, P., Wegscheider, K., Schwartz, K., Brito, D. *et al.* (2009) A new polymorphism in human calmodulin III gene promoter is a potential modifier gene for familial hypertrophic cardiomyopathy. *Eur. Heart J.*, **30**, 1648–1655.

57. Charron, P., Dubourg, O., Desnos, M., Bouhour, J.B., Isnard, R., Hagège, A., Carrier, L., Bonne, G., Tesson, F., Richard, P. *et al.* (1998) Diagnostic value of electrocardiography and echocardiography for familial hypertrophic cardiomyopathy in genotyped children. *Eur. Heart J.*, **19**, 1377–1382.

58. Muller, O.J., Schinkel, S., Kleinschmidt, J.A., Katus, H.A. and Bekeredjian, R. (2008) Augmentation of AAV-mediated cardiac gene transfer after systemic administration in adult rats. *Gene. Ther.*, **15**, 1558–1565.

59. Neagoe, C., Kulke, M., del Monte, F., Gwathmey, J.K., de Tombe, P.P., Hajjar, R.J. and Linke, W.A. (2002) Titin isoform switch in ischemic human heart disease. *Circulation*, **106**, 1333–1341.

60. Pohlmann, L., Kroger, I., Vignier, N., Schlossarek, S., Kramer, E., Coirault, C., Sultan, K.R., El-Armouche, A., Winegrad, S., Eschenhagen, T. *et al.* (2007) Cardiac myosin-binding protein C is required for complete relaxation in intact myocytes. *Circ. Res.*, **101**, 928–938.

61. Bardswell, S.C., Cuello, F., Rowland, A.J., Sadayappan, S., Robbins, J., Gautel, M., Walker, J.W., Kentish, J.C. and Avkiran, M. (2010) Distinct sarcomeric substrates are responsible for protein kinase D-mediated regulation of cardiac myofilament Ca2+ sensitivity and cross-bridge cycling. *J. Biol. Chem.*, **285**, 5674–5682.

62. Hansen, A., Eder, A., Bonstrup, M., Flato, M., Mewe, M., Schaaf, S., Aksehirlioglu, B., Schworer, A., Uebeler, J. and Eschenhagen, T. (2010) Development of a drug screening platform based on engineered heart tissue. *Circ. Res.*, **107**, 35–44.

63. Schaaf, S., Shibamiya, A., Mewe, M., Eder, A., Stohr, A., Hirt, M.N., Rau, T., Zimmermann, W.H., Conradi, L., Eschenhagen, T. *et al.* (2011) Human engineered heart tissue as a versatile tool in basic research and preclinical toxicology. *PLoS One*, **6**, e26397.